*Quaternary Research* (2023), **113**, 87–104
doi:10.1017/qua.2022.70

## Research Article

# Terrestrial ecosystem transformations in response to rapid climate change during the last deglaciation around Mono Lake, California, USA

Adam J. Benfield[a*], Sarah J. Ivory[a,b], Bailee N. Hodelka[c], Susan R.H. Zimmerman[d,e] and Michael M. McGlue[c]

[a]Department of Geosciences, The Pennsylvania State University, University Park, PA, 16802, USA; [b]Earth and Environmental Systems Institute, Pennsylvania State University, University Park, PA, 16802, USA; [c]Department of Earth and Environmental Sciences, University of Kentucky, Lexington, KY, 40508, USA; [d]Berkeley Geochronology Center, Berkeley, CA 94709, USA and [e]Center for Accelerator Mass Spectrometry, Lawrence Livermore National Laboratory, Livermore, CA, 94550, USA

### Abstract

We examine major reorganizations of the terrestrial ecosystem around Mono Lake, California during the last deglacial period from 16,000–9,000 cal yr BP using pollen, microcharcoal, and coprophilous fungal spores (*Sporormiella*) from a deep-water sediment core. The pollen results record the assemblage, decline, and replacement of a mixed wooded community of Sierran and Great Basin taxa with Alkali Sink and Sagebrush Steppe biomes around Mono Lake. In particular, the enigmatic presence of *Sequoiadendron*-type pollen and its extirpation during the early Holocene hint at substantial biogeographic reorganizations on the Sierran-Great Basin ecotone during deglaciation. Rapid regional hydroclimate changes produced structural alterations in pine–juniper woodlands facilitated by increases in wildfires at 14,800 cal yr BP, 13,900 cal yr BP, and 12,800 cal yr BP. The rapid canopy changes altered the availability of herbaceous understory plants, likely putting pressure on megafauna populations, which declined in a stepwise fashion at 15,000 cal yr BP and 12,700 cal yr BP before final extirpation from Mono Basin at 11,500 cal yr BP. However, wooded vegetation communities overall remained resistant to abrupt hydroclimate changes during the late Pleistocene; instead, they gradually declined and were replaced by Alkali Sink communities in the lowlands as temperature increased into the Early Holocene, and Mono Lake regressed.

**Keywords:** Sierra Nevada, Great Basin, Pleistocene, Megafauna Extinction, Abrupt Climate Change, Giant Sequoia

(Received 24 June 2022; accepted 23 November 2022)

## INTRODUCTION

The last major reorganization of terrestrial ecosystems in California occurred during the last glacial termination (Glover et al., 2021), a period of large and often rapid climate oscillations (Denton et al., 2010; Clark et al., 2012). A succession of abrupt climate-change events during deglaciation have been well-documented in the Northern Hemisphere: Henrich Stadial 1, the Bølling and Allerød interstadials, and the Younger Dryas, all of which significantly overprinted long-term, orbitally paced warming with excursions of 1–2°C over decades to centuries (Denton et al., 2010). Paleoecological studies from eastern North America, where there is a robust network of multiproxy, high-resolution paleoecological studies, have applied a conceptual framework for interpretating feedback among fire, vegetation, and megafauna using well-resolved records of charcoal, pollen, and coprophilous fungal spores (e.g., Shuman et al., 2009; Gill et al., 2009, 2012; Oswald et al., 2018). Those studies have demonstrated that rapid climate and environmental changes of the last deglaciation produced profound, long-term effects on vegetation composition and structure, fire regimes, and megafauna populations.

Fewer studies have examined the ecological feedbacks among fire, vegetation, and megafauna using microfossils from the sedimentary record during deglaciation in the western USA (e.g., Davis and Shafer, 2006). The western US has a complex history of environmental change as gradually reducing moisture shrank the massive pluvial lakes of the Great Basin, giving rise to the semiarid modern landscape (Grayson, 2011). Paleoclimate evidence, largely from speleothem and pluvial lake-shoreline reconstructions, has shown that terrestrial environments were intimately connected to Pacific and North Atlantic Ocean conditions during glacial terminations (Oster et al., 2009, 2015; Lyle et al., 2010; Lachniet et al., 2014; Hudson et al., 2019), implying that terrestrial ecosystems would have experienced major environmental swings during deglaciation. Yet, a persistent problem in late Quaternary paleoecology of the western USA has been the muted or uncertain response of vegetation and fire regimes to deglacial climate-change events (e.g., Younger Dryas, MacDonald et al., 2008).

However, the longer-term assembly of the terrestrial ecosystems of the central Sierra Nevada (Cole, 1983; Davis et al., 1985; Anderson, 1990a; Smith and Anderson, 1992; Anderson

*Corresponding author email address: ajbenfield@psu.edu

**Cite this article:** Benfield AJ, Ivory SJ, Hodelka BN, Zimmerman SRH, McGlue MM (2023). Terrestrial ecosystem transformations in response to rapid climate change during the last deglaciation around Mono Lake, California, USA. *Quaternary Research* **113**, 87–104. https://doi.org/10.1017/qua.2022.70

and Smith, 1994; Koehler and Anderson, 1994) and western Great Basin (Batchelder, 1970; Jennings and Elliott-Fisk, 1993; Nowak et al., 1994; Woolfenden, 2003; Mensing, 2001; Mensing et al., 2008; Brugger and Rhode, 2020) since the late Pleistocene are documented by a rich history of Quaternary subfossil pollen and macrofossil studies from lakes, wetlands, and middens. This work has shown that much of the Sierra Nevada and Great Basin was covered in a subalpine community of *Artemisia*-, *Pinus*-, *Abies*-, and *Juniperus*-dominated woodlands that transitioned during the Holocene to more altitudinally stratified montane forests, chaparral/woodlands, and open lowland steppes. The interglacial transition initiated biogeographic shifts in the distribution of plants over 100s of kilometers, including iconic, keystone species such as *Pinus monophylla* (single-leaf pinyon pine; Cole et al., 2013), *Juniperus scopulorum* (Rocky Mountain juniper; Woolfenden, 2003), and *Sequoiadendron giganteum* (giant sequoia; Cole, 1983).

Despite the extensive paleoecological work conducted in the Sierra Nevada and the Great Basin, very few pollen studies have had the sampling resolution necessary to detect more rapid events (<250 years per sample, after Anderson et al., 2022). Instead, most ecological interpretations in the region have centered on responses to gradual, orbitally forced climate change (e.g., Davis et al., 1985; Anderson, 1990a; Anderson and Smith, 1994), rather than more rapid and nonlinear events (e.g., Heusser et al., 2015; Glover et al., 2020; Zimmerman and Wahl, 2020). More recent investigations (Mensing, 2001; MacDonald et al., 2008; Oster et al., 2009; 2015; Heusser et al., 2015; Ali, 2018) have shown hydroclimatic sensitivity to rapid change, but the ecological response remains poorly understood, particularly east of the Sierra Crest (Anderson et al., 2022; Fig. 1).

The wooded landscape of the Pleistocene Great Basin and Sierra Nevada also supported at least 19 genera of now-extinct mammals until the terminal Pleistocene, with horses, camels, and mastodons being the most common (Grayson, 2006). One paleoecological study (Davis and Shafer, 2006) employed coprophilous fungal spores as a proxy for megafauna activity within depositional basins from around the western US and showed that Pleistocene landscapes typically supported populations of the Rancholabrean Pleistocene megafauna until after 12,900 cal yr BP (calibrated years before present, AD 1950). Another study by Mack and Thompson (1982) suggested that the Great Basin supported Pleistocene megafauna in relatively low populations densities. Yet, more recent work has modeled dense populations of at least some megafauna (e.g., *Bison* spp.; Wendt et al., 2022) that were also sensitive to the abrupt warming of the Bølling Interstade and the onset of the Holocene. The causes of the megafauna extinction in the western US continued to be debated, but vegetation change has been invoked as a major driver of extinction (Grayson, 2016).

To understand the history of semiarid terrestrial ecosystems and their response to major environmental change, we present a new record of vegetation, fire, and megafauna presence surrounding Mono Lake from ca. 16,000–9,000 cal yr BP using pollen, microcharcoal, and spores of the coprophilous fungus *Sporormiella*. Mono Lake provides an ideal study site to examine how terrestrial ecosystems were shaped by climate change because it sits at the ecotone of the Great Basin floristic province and the central Sierra Nevada (Fig. 1). Mono Lake also has well-dated paleohydrologic reconstructions from sediment cores and relict shorelines, allowing us to understand coupled ecosystem and hydroclimate interactions over this key interval (Ali, 2018; Ali et al., 2022). The pollen results show a gradual decline in woodlands around Mono Lake, punctuated by rapid infilling or opening of woodlands during periods of rapid change during the late Pleistocene. The rapid changes in canopy openness and increases in wildfire appear to have had the greatest effect on megafauna activity in the basin because *Sporormiella* abundances decline at periods of enhanced vegetation turnover and microcharcoal peaks.

## Study setting

Mono Lake is a large, closed-basin lake at the western edge of the Great Basin and the eastern flank of the Sierra Nevada, California, at 1945 m above sea level (m asl; Fig. 1). Diversion of major inflowing rivers associated with the Los Angeles aqueduct system reduced water-level elevation and created hypersaline conditions in Mono Lake beginning in the mid-twentieth century (Jellison and Melack, 1993). Mono Basin is surrounded by highlands, with the Sierra Nevada mountains to the west, the Bodie Hills to the north, the Granite and Cowtrack mountains to the east, and the Mono-Inyo Craters and Glass Mountain to the south. Mean annual precipitation near the western shore is ~400 mm $yr^{-1}$ and decreases toward the eastern part of the basin. The majority of precipitation is snowfall from November–March, and the lake is primarily fed by short creeks transporting snowmelt from the eastern Sierra Nevada (Fig. 1B). The Kootzaduka'a people ("eaters of the brine fly"), hunter-gatherers of the Northern Paiute language group, have lived in Mono Basin since at least the early Late Holocene (Brady, 2011). Regional archaeological evidence suggests low human populations surrounding Mono Lake and Bodie Hills during the Early Holocene as compared to other Great Basin lakes, but they increased during the Middle to Late Holocene (Halford, 1998; Brady, 2011). Modern megafauna in or nearby to the Mono Basin include *Odocoileus hemionus* (mule deer), *Ovis canadensis sierrae* (Sierra Nevada bighorn sheep), *Equus ferus caballus* (feral horses), and *Puma concolor* (mountain lions).

Modern vegetation communities within the Mono Basin form along altitudinal zones, soil types, and precipitation gradients (Winkler, 1977; Constantine, 1993). Alkali Sink steppe dominated by *Sarcobatus vermiculatus* (greasewood; Amaranthaceae), *Atriplex* spp. (saltbush; Amaranthaceae), *Chrysothamnus nauseosus* (rubber rabbitbrush; Asteraceae), and *Distichlis spicata* (saltgrass; Poaceae) surrounds the lake. Littoral Cyperaceae-dominated marshes occur in flat-lying areas and near deltas. At slightly higher elevations on less saline soils, steppe of *Artemisia tridentata* (big sage; Asteraceae), *Purshia tridentata* (bitterbrush; Rosaceae), *Ephedra viridis* (Mormon tea; Ephedraceae), and *Eriogonum* spp. (buckwheat; Polygonaceae) occur below 2000 m asl. Several stand-replacing fires have occurred in the steppe around the south shore of Mono Lake over the last 30 years, leaving barren or grass-dominated patches. Riparian zones dominated by *Salix exigua* (coyote willow; Salicaceae), *Populus trichocarpa* (black cottonwood; Salicaceae), and *Populus tremuloides* (quaking aspen; Salicaceae) occur in the eastern creeks draining the Sierra Nevada (Constantine, 1993).

On the flank of the Sierra Nevada and Bodie Hills, woodlands of *Pinus monophylla* (single-leaf pinyon pine; Pinaceae) and to a lesser extent *Juniperus osteosperma* (Utah juniper; Cupressaceae) are interspersed with shrubs of *Cercocarpus ledifolius* (mountain mahogany; Rosaceae), *Artemisia*, *Eriogonum* spp., *Ceanothus* sp. (Rhamnaceae), and *Ephedra* (Constantine, 1993), while a pure stand of *J. osteosperma* is found on sandy dunes of the western

https://doi.org/10.1017/qua.2022.70 Published online by Cambridge University Press

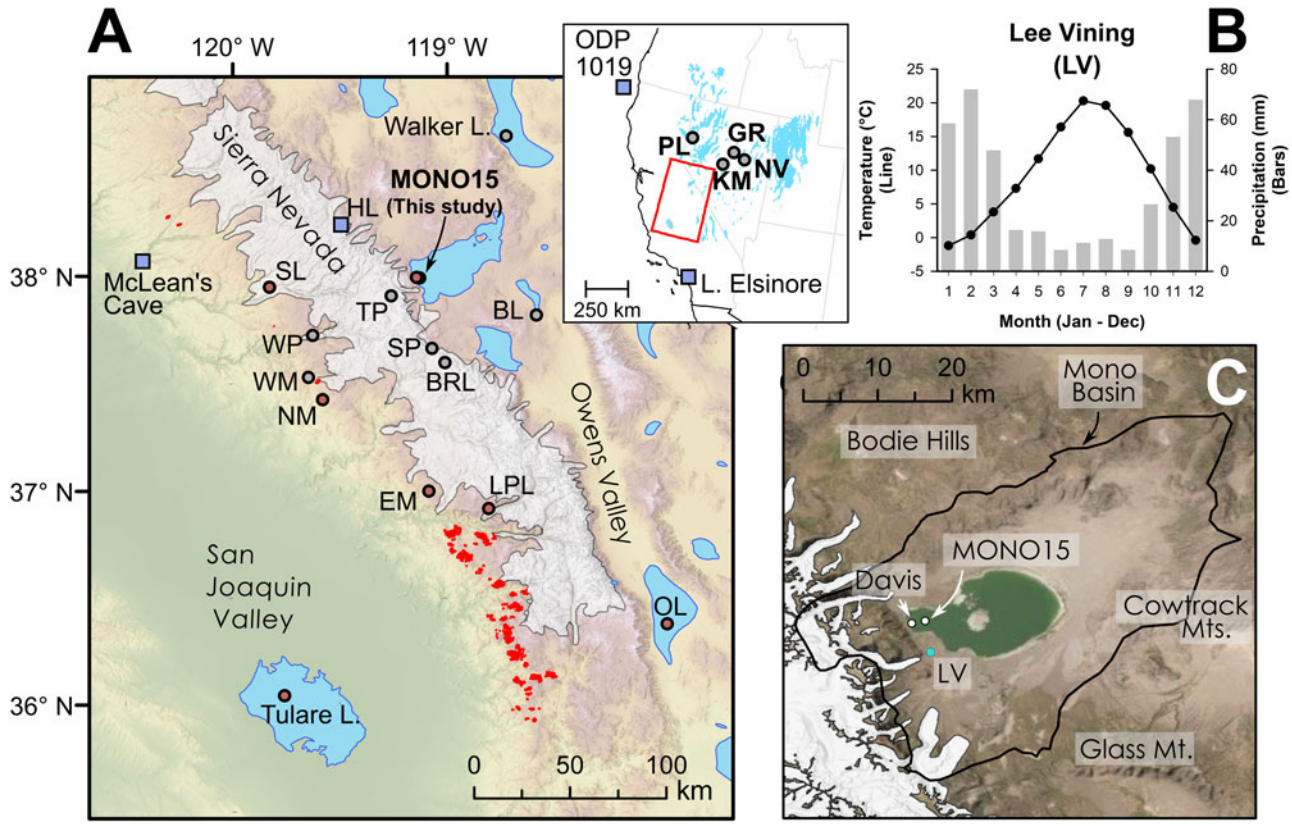


**Figure 1.** (A) Regional map showing location of late Pleistocene lakes, glaciers, and prior studies. Circles show location of pollen or other paleoecological study sites and squares show locations of paleoclimate proxies mentioned in the text. Modern *Sequoiadendron* groves are shown in red, and red circles indicate site locations with late Pleistocene *Sequoiadendron* pollen. Inset shows location of study region (red rectangle) and ODP Site 1019 (Barron et al., 2003; Praetorius et al., 2020), Lake Elsinore (Kirby et al., 2013; Feakins et al., 2019), and Great Basin core-based pollen studies. (B) Data for climate normals (1981–2010) of seasonal records of precipitation (bars) and temperature (line) from Lee Vining, California (https://www.ncdc.noaa.gov/cdo-web/ accessed 4/25/20). (C) Modern Mono Lake and surroundings with coring locations of MONO15 (this study) and Davis (1999a). Image from Google Earth. White shading the greatest extent of Tioga glaciers in A and C from Gillespie and Clark (2011) and Wahrhaftig et al. (2019), respectively. BL—Black Lake, BRL—Barrett Lake, EM—Exchequer Meadows, GR—Gund Ranch, HL—Hidden Lake, KM—Kingston Meadow, LPL—Lilypad Lake, NM—Nicholas Meadows, NV—Newark Valley Pond, OL—Owens Lake, PL—Pyramid Lake, SP—Starkweather Pond, SL—Swamp Lake, TP—Tioga Pass Pond, WM—Wawona Meadow, WP—Woski Pond.

Mono Basin. Substantial portions of the eastern pinyon–juniper woodlands were also burned by the Marina fire in 2016, completely killing the stands. Forests of fire-adapted *Pinus jeffreyi* (Jeffrey pine; Pinaceae) with *Purshia tridentata* understories occur around Mono Craters and Glass Mountain (Anderson and Davis, 1988; Millar et al., 2006). Within the eastern Sierra Nevada, pinyon–juniper woodlands and Jeffrey pine dominate from ~2000 m to 2300 m. Montane forests characterized by *Pinus contorta* subsp. *murrayana* (Sierra lodgepole pine; Pinaceae), *Abies magnifica*, and *Abies concolor* (red fir and white fir, respectively; Pinaceae) extend from 2300 to 2500 m. Subalpine forests characterized by *Tsuga mertensiana* (mountain hemlock; Pinaceae) occur up to 3000 m (Anderson and Davis, 1988; Barbour et al., 2007). Although not found within the Mono Basin, *Quercus vacciniifolia* and *Q. chrysolepis* (huckleberry oak and canyon live oak, respectively; Fagaceae) are found on dry hillslopes in the eastern Sierra Nevada (Anderson and Davis, 1988) and *Corylus cornuta* var. *californica* (California hazelnut) is a shrub characteristic of Sierran montane forests (Anderson and Davis, 1988; Barbour et al., 2007). Small, distinct groves of *Sequoiadendron* (giant sequoia; Pinaceae) grow in the western Sierra Nevada interspersed within Sierra montane forests (Hartesveldt et al., 1975).

Anderson and Davis (1988) first analyzed modern pollen samples along a transect across the central Sierra Nevada stretching from Yosemite to nearby Mono Lake. Their work recognized distinct pollen zones along altitude, reflecting changes in vegetation due to the strong climate gradients of the Sierra Nevada (Fig. 2) despite an overall low pollen taxonomic diversity and an overrepresentation of *Pinus* pollen. The cool and wet Sierran montane and subalpine zones are dominated by *Pinus*, *Abies*, *Tsuga mertensiana* pollen on both sides of the Sierra Crest (Anderson and Davis, 1988; Barbour et al., 2007). On the drier eastern flank, *Pinus* and *Artemisia* pollen are most common. Within the Great Basin, there is an acute lack of modern pollen samples (Minckley et al., 2008), but existing modern pollen work (Solomon and Silkworth, 1986; Anderson and Davis, 1988; Woolfenden, 2003) showed large differences in Cupressaceae abundance, probably reflecting the strong spatial heterogeneity of *Juniperus* woodlands in Mono Basin (Constantine, 1993) and throughout the Great Basin (Romme et al., 2009).

Mono Basin has well-preserved sedimentary and geomorphological records of the late Quaternary that were first investigated by Russell (1889) and later by Putnam (1950), Lajoie (1968), Stine (1990), Benson et al. (1998), Davis (1999a), and Zimmerman et al. (2011a, b). More recently, Ali (2018) and Ali et al. (2022) refined and re-dated paleoshorelines using uranium-series dating, and created a well-dated late Quaternary hydrograph for Mono Lake. The Pleistocene Lake in the Mono

https://doi.org/10.1017/qua.2022.70 Published online by Cambridge University Press

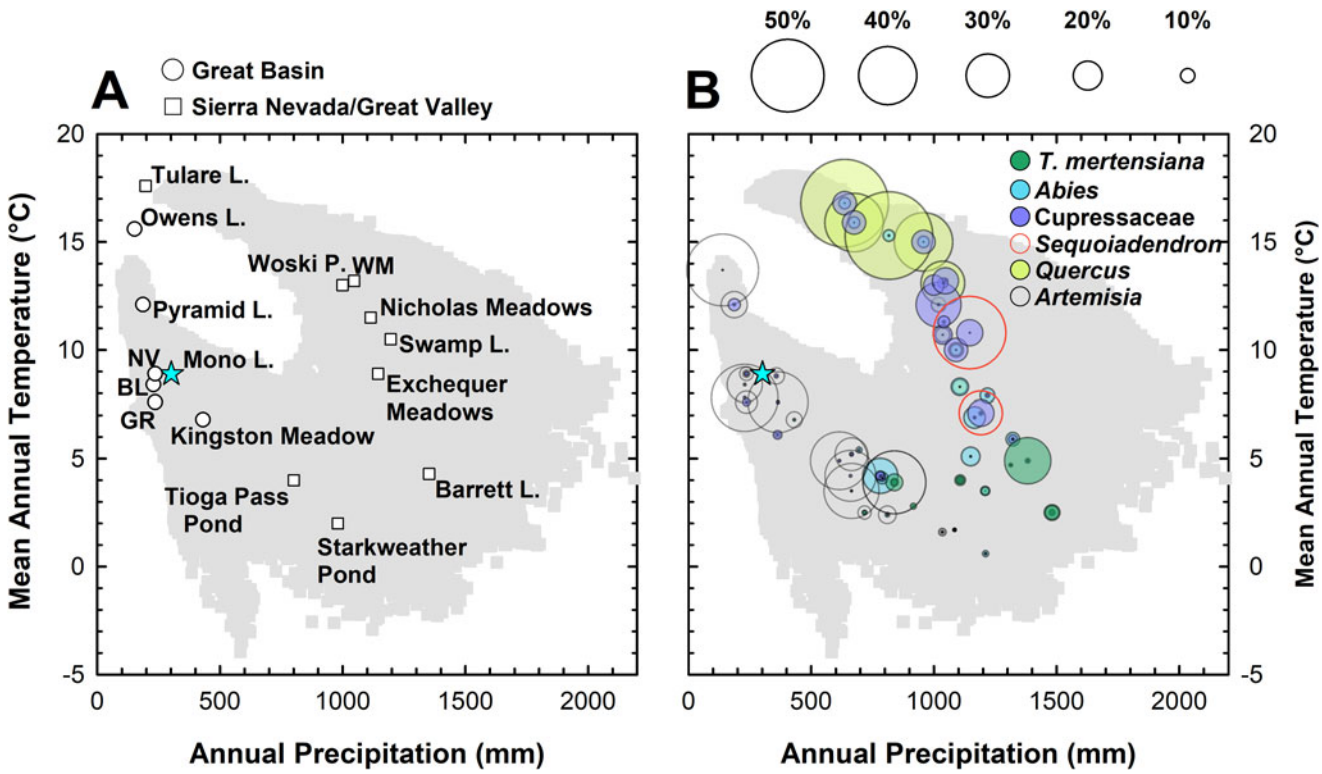


**Figure 2.** Graphs showing relationship between modern precipitation and mean annual temperature in the central Sierra Nevada and Great Basin. Gray squares show 30-yr climate normals (1991–2020) at 800 $m^2$ resolution (PRISM Climate Group, 2014). (A) "Climate-space" location of regional paleoecological studies mentioned in the text (Table 1). Blue star denotes climate-space of the western embayment of Mono Lake (this study). (B) Plot shown in (A) with superimposed bubble plots showing percent abundance of indicator pollen taxa (*Artemisia*, *Quercus*, Cupressaceae, *Sequoiadendron*-type, *Abies*, and *Tsuga mertensiana*) from surface sediment samples (Batchelder, 1970; Anderson and Davis, 1988; Anderson, 1990a; Whitmore et al., 2005). *Pinus* pollen abundances are not shown for legibility but are typically above 75% of the terrestrial pollen sum between 1000 mm and 1500 mm annual precipitation. NV—Newark Valley Pond, BL—Black Lake, GR—Gund Ranch, WM—Wawona Meadow.

Basin, named Lake Russell in honor of Israel Russell, covered nearly the entire Mono Valley at its deglacial-aged highstand (Lajoie, 1968; Ali, 2018; Fig. 1). For simplicity, we refer to the lake in the Mono Basin as Mono Lake regardless of time or size. During the last deglacial period, Mono Lake waxed and waned considerably in depth and spatial extent as it was influenced by major climate-change events during the glacial termination before regressing to approximately its pre-diversion size during the Early Holocene (Ali, 2018).

Paleoecological studies in the Mono Basin have been more limited. Davis (1999a) presented a core-based pollen record collected from the littoral zone of the western embayment (Fig. 1C). His record, which spanned from 13,000 cal yr BP to present, showed the greatest turnover in pollen taxa during the terminal Pleistocene, when Cupressaceae and *Sequoiadendron*-type pollen declined and were replaced by modern vegetation assemblages.

## MATERIALS AND METHODS

The sediment core UWI-MONO15-1C/D (hereafter MONO15) was extracted in 2015 from the western embayment of Mono Lake (37.994°N, 119.125°W; 1945 m asl; Fig. 1C) in 18-m water depth (Hodelka et al., 2020). Here, we present an age-depth model based on 23 accelerator mass-spectrometry radiocarbon dates, measured from plant macrofossils, charcoal, pollen purified by flow cytometry, and four tephra correlations (Hodelka et al., 2020; Tunno et al., 2021; Zimmerman et al., 2021; Table 1). Our Bacon age-depth model has been updated from the previous MONO15 age model presented by Hodelka et al. (2020) by including four new radiocarbon dates conducted for this study (Table 1). The radiocarbon ages and tephra age constraints were used as input for the R package Bacon version 2.5.7 software program that uses the IntCal20 calibration curve to convert radiocarbon ages to calibrated ages before present (AD 1950). Periods of instantaneous sedimentation caused by sediment slumps and turbidite deposits as interpreted by Hodelka et al (2020) based on visual lithologic description of the MONO15 core, were also used as input (Fig. 3). Based on these stratigraphic and chronologic constraints, the Bacon package constructed a Bayesian age-depth model (Blaauw and Christen, 2011; R Core Team, 2022) which is very similar (<500 years difference) to the original Hodelka et al. (2020) model.

A total of 58 sediment aliquots 1-cm thick and 1–2 ml in volume were subsampled for palynological analysis from the MONO15 core, including 57 samples from 376 cm to 984 cm composite-core depth, and one core-top surface sediment pollen sample. Sediment subsamples were acidified with 10% HCl. and one tablet of exotic *Lycopodium* spores was added to each sample. Clay minerals were dispersed by soaking samples in 1% sodium hexametaphosphate solution and agitating for 24 hours. An enzymatic solution was used to clean organic matter from palynomorph grains following the procedures of O'Keefe and Wymer (2017), modified from Schols et al. (2004). Palynomorphs were extracted from mineral sediments via density separation using the heavy liquid lithium heteropolytungstate (LST) at 2.0 specific gravity. Residues were then stained with safranin, and stored in glycerin at the Penn State Pollen Lab.

https://doi.org/10.1017/qua.2022.70 Published online by Cambridge University Press

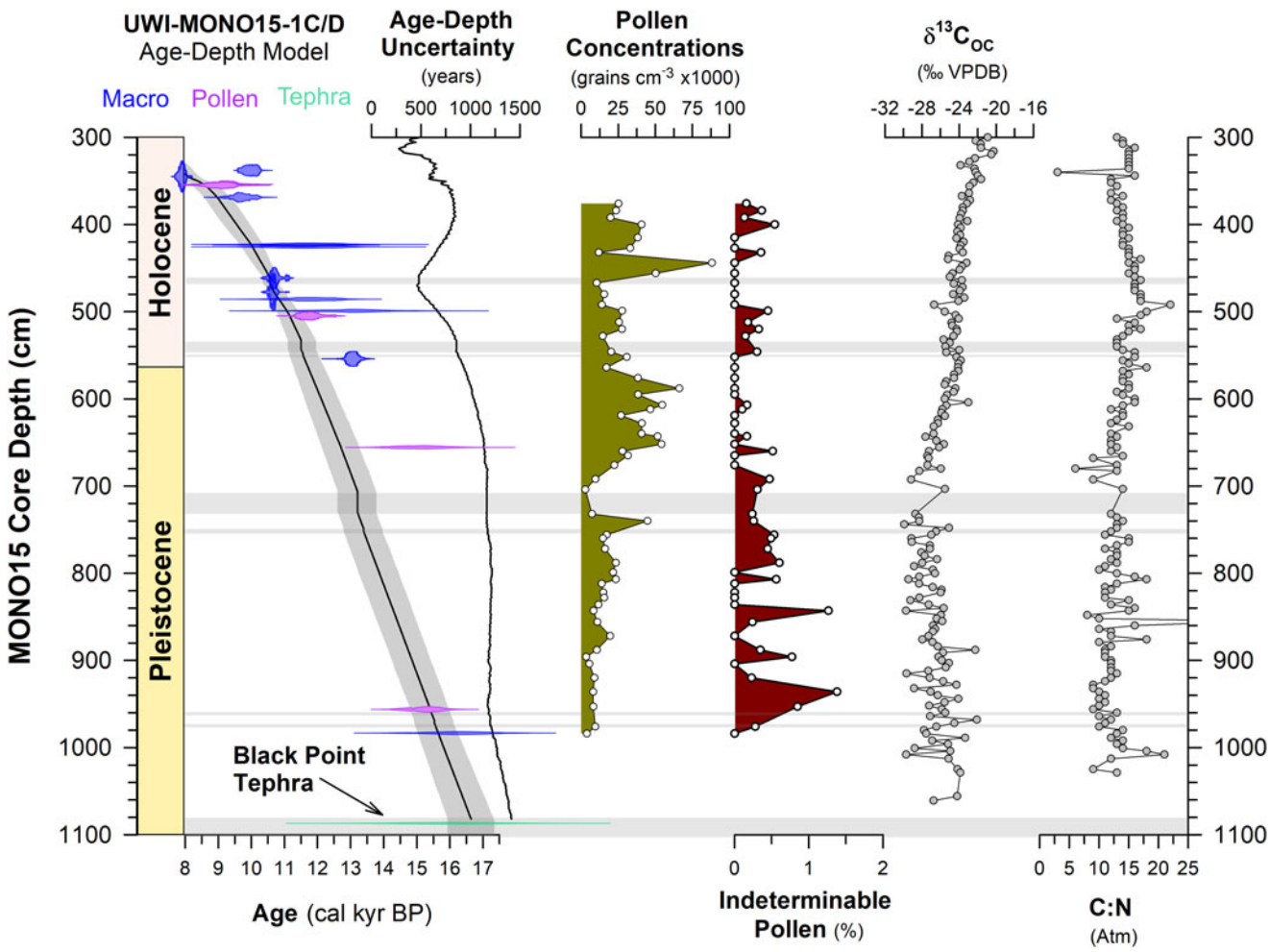


**Figure 3.** Bacon age-depth model updated from Hodelka et al. (2020), with pollen concentrations (this study), percentage of indeterminable pollen grains (this study), $\delta^{13}C_{OC}$ (Hodelka et al., 2020; VPDB—Vienna PeeDee Belemnite), and C:N values (Hodelka et al., 2020) of UWI-MONO15 sediments from 300–1100 cm composite core depth. Age-control points for the Bacon age-depth model are shown as mirrored probability density functions of the 2-σ calibrated age-range for each date. Probability density functions show dates from terrestrial plant macrofossils (macro; blue), purified pollen extracts (pollen; purple), and tephra correlations (tephra; teal). The black solid line shows the mean age from the Bacon age model with gray shading showing 95% confidence intervals. Horizontal light gray bars show slumps of instantaneous sediment deposition added to the age-depth model based on core observations of tephra and turbidites (after Hodelka et al., 2020).

A minimum of 300 terrestrial pollen grains were counted for each sample, including at least 100 non-*Pinus* terrestrial pollen grains. Palynomorph identification was made using published keys and papers (McAndrews et al., 1973; Davis, 1999a, b; Kapp et al., 2000) and a reference slide collection at the Penn State Pollen Lab. *Sequoiadendron*-type pollen was differentiated from Cupressaceae grains by the presence of a papilla (after Davis, 1999a; Supplemental Figure S3). Pollen percentages were determined by dividing by the sum of all terrestrial pollen types. The percentages of *Sporormiella* fungal spores, Cyperaceae, and other aquatic pollen types were calculated against a sum of all terrestrial pollen. Palynomorph concentrations (grains/cm$^3$) and influx rates (grains/cm$^2$/yr) were calculated for each taxon after Faegri et al. (1989). Microcharcoal particles (<250 µm size fraction) were counted on the same sample slides during pollen identification. Concentrations and accumulation rates of microcharcoal were calculated using the same method as pollen grains.

Pollen zones were defined using stratigraphically constrained incremental sum of squares cluster analysis (CONISS; Grimm, 1987) using the R package *vegan* version 2.5.7 (Oksanen et al., 2019; Supplemental Figure 4). To highlight ecological gradients, we used detrended correspondence analysis (DCA) using the R package *vegan* (Oksanen et al., 2019). The analysis was performed on Wisconsin double standardization percentage data on all non-singleton pollen taxa (Supplemental Table 2S). A DCA score was obtained for the surface-sediment pollen sample by passively projecting it using the *vegan* package onto the ordination generated using the subfossil data. Regional core-top pollen abundances used to create Figure 7 were obtained from the Neotoma Paleoecological Database (Williams et al., 2018) and original published sources (Table 2). Lake surface areas presented in Table 1 were estimated with Google Earth or synthesized from the source publication.

## RESULTS

### *Core lithology and chronology*

The lithology of the MONO15 core was previously described by Hodelka et al. (2020). Briefly, the core consists of well-preserved

https://doi.org/10.1017/qua.2022.70 Published online by Cambridge University Press

**Table 1.** Radiocarbon ($^{14}$C) data ($n = 23$) and other ($n = 4$) control points used in the age-depth model for core UWI-MONO15-1C/D. †New radiocarbon dates not presented by Hodelka et al. (2020). *Dates from tephra from BINGO-MONO10-4A core were acquired via $^{14}$C AMS dating and discussed in Hodelka et al. (2020) and Zimmerman et al. (2021).

| CAMS # | Composite depth (cm) | Material | $^{14}$C age (yr) | $^{14}$C age uncertainty (yr) | Median age (cal yr BP) | 2-σ range (cal yr BP) |
|---|---|---|---|---|---|---|
| 177423 | 205 | Plant macro | 3775 | 40 | 4147 | 3987–4290 |
| n/a | 224 | Tephra* | 4365 | 85 | 4974 | 4823–5294 |
| n/a | 228 | Tephra* | 4700 | 450 | 5344 | 4227–6354 |
| n/a | 234 | Tephra* | 5065 | 610 | 5766 | 4286–7168 |
| 176259 | 296.3 | Plant macro | 5740 | 30 | 6536 | 6447–6632 |
| 173692 | 307.4 | Plant macro | 6300 | 70 | 7216 | 7004–7339 |
| 173693 | 314 | Plant macro | 6350 | 45 | 7200 | 7080–7350 |
| 173695 | 314 | Plant macro | 6150 | 40 | 7052 | 6937–7163 |
| 177425 | 316.4 | Plant macro | 6620 | 110 | 7504 | 7315–7677 |
| 176260 | 337 | Charcoal | 8850 | 100 | 9926 | 9654–10198 |
| 173694 | 344 | Plant macro | 7070 | 70 | 7889 | 7742–8016 |
| 178075 | 353 | Pollen | 8220 | 240 | 9146 | 8535–9680 |
| 118472 | 354 | Pollen | 8140 | 240 | 9053 | 8514–9538 |
| 176261 | 367.7 | Plant macro | 8610 | 180 | 9659 | 9264–10188 |
| 177392 | 421.5 | Plant macro | 10070 | 570 | 11659 | 10193–13093 |
| 177393 | 422.2 | Plant macro | 9910 | 410 | 11465 | 10373–12675 |
| 177394 | 424.3 | Plant macro | 10010 | 570 | 11584 | 10152–13082 |
| 177395 | 459.8 | Plant macro | 9400 | 70 | 10630 | 10407–11066 |
| 185680† | 475.8 | Plant macro | 9365 | 40 | 10583 | 10495–10698 |
| 186446† | 484 | Plant macro | 10070 | 410 | 11693 | 10556–12749 |
| 177396 | 497.3 | Plant macro | 11110 | 600 | 12966 | 11228–14479 |
| 178076 | 503 | Pollen | 10090 | 130 | 11654 | 11235–12103 |
| 186447† | 552 | Plant macro | 11030 | 150 | 12953 | 12728–13179 |
| 178074 | 653 | Pollen | 12650 | 390 | 14946 | 13749–16114 |
| 179010 | 952 | Pollen | 12740 | 220 | 15138 | 14230–15787 |
| 186998† | 979 | Plant macro | 13400 | 500 | 16120 | 14767–17487 |
| n/a | 1082 | Tephra | n/a | n/a | 16430 | 15590–17070 |

lacustrine muds interbedded with occasional tephras and sand layers. Late Pleistocene units contain inclusions of pebbles that penetrate bedding, and were interpreted as dropstones (Hodelka et al., 2020). Sediments that span the terminal Pleistocene to Holocene transition show a shift from finely laminated silts with high organic-matter content to laminated muds with occasional thinly bedded turbidites, likely reflecting the Early Holocene regression from a Younger Dryas highstand (Ali, 2018). Holocene sediments contain finely laminated calcareous muds with less siliciclastic detritus, indicative of a low-energy depositional environment in a shallower lake (Hodelka et al., 2020).

Fourteen radiocarbon ages cover the interval of pollen sampling from 15,700–9,100 cal yr BP (984–376 cm core depth; Fig. 3). There was paucity of terrestrial plant macrofossils between 952 cm and 653 cm depth, leading to a gap of 3 m and 2,700 years in the age control points. However, the basal age of the MONO15 core is well-constrained by an altered basaltic tephra inferred to derive from a late eruption of the Black Point volcano (17,000–14,600 cal yr BP; Bailey, 2004) and two radiocarbon dates at 979 cm and 952 cm composite depth, respectively. Modeled age-depth uncertainties averaged ± 500 years in the Pleistocene, while more plant macrofossils were available for generating dates from the terminal Pleistocene and early Holocene, increasing the precision during the Early Holocene to an average of ± 350 years. The average temporal resolution between pollen samples is 100 ± 40 years/sample for the Pleistocene, and 145 ± 60 years/sample for the Early Holocene. Overall sedimentation rates indicate each 1-cm-thick pollen aliquot integrated 10 ± 0.4 years of time during the Pleistocene and 14 ± 4 years during the Early Holocene.

### *Palynological record and statistical analysis*

The pollen record from the MONO15 core is divided into seven pollen zones: A (984–888 cm), B (888–822 cm), C1 (822–756 cm),

https://doi.org/10.1017/qua.2022.70 Published online by Cambridge University Press

**Table 2.** Modern pollen samples from the central Sierra Nevada and Great Basin used to construct Figure 7. P is *Pinus*, C is Cupressaceae, and A is *Artemisia*. *Indicates surface areas estimated from Google Earth; other surface areas given in original reference.

| Site name | Region | Vegetation | Surface area ($km^2$) | Pollen% | | | References |
|---|---|---|---|---|---|---|---|
| | | | | P | C | A | |
| Black Lake (BL) | Great Basin | Alkali sink, sagebrush and juniper | 0.4* | 80 | 4 | 9 | Batchelder 1970; Benfield, A.J., unpublished data |
| Gund Ranch (GR) | Great Basin | sagebrush | 0.4* | 30 | 0 | 25 | Brugger and Rhode, 2020 |
| Kingston Meadow (KM) | Great Basin | sagebrush and minor juniper | 0.01* | 14 | 0 | 25 | Mensing et al., 2008 |
| Mono Lake (ML) | Great Basin | Alkali sink, sagebrush and juniper | 150 | 50 | 3 | 11 | Davis, 1999a |
| Newark Valley Pond (NV) | Great Basin | sagebrush and minor juniper | 0.01* | 17 | 7 | 23 | Mensing et al., 2008 |
| Owens Lake (OL) | Great Basin | Alkali sink | 290 | 31 | <1 | 2 | Woolfenden, 2003 |
| Pyramid Lake (PL) | Great Basin | Alkali sink, sagebrush, and juniper | 450* | 28 | 7 | 17 | Mensing et al., 2008 |
| Barrett Lake (BL) | Sierra Nevada | Upper Sierran Montane | 0.03 | 79 | 4 | <1 | Anderson, 1990a |
| Exchequer Meadows (EM) | Sierra Nevada | Upper Sierran Montane | 0.1* | 50 | 1 | <1 | Davis and Moratto, 1988 |
| Nicholas Meadows (NM) | Sierra Nevada | Sierran Montane, *C. decurrens* | 2.2 | 39 | 39 | 0 | Koehler and Anderson, 1994 |
| Starkweather Pond (SP) | Sierra Nevada | Upper Sierran Montane, *J. occidentalis* | 0.02 | 76 | 6 | 3 | Anderson, 1990a |
| Swamp Lake (SL) | Sierra Nevada | Sierran Montane, *C. decurrens* | 0.08 | 60 | 21 | 0 | Smith and Anderson, 1992 |
| Tulare Lake (TL) | Great Valley | Alkali sink, grassland and oak savanna | 1900 | 11 | <1 | 4 | Davis 1999b |
| Wawona Meadow (WM) | Sierra Nevada | Sierran Montane, *C. decurrens* | 0.4 | 45 | 20 | 0 | Anderson and Stillick, 2013 |
| Woski Pond (WP) | Sierra Nevada | Sierran Montane, *C. decurrens* | 0.1 | 47 | 14 | 2 | Anderson and Carpenter, 1991 |

C2 (756–652 cm), D (652–528 cm), E1 (528–456 cm), and E2 (456–376 cm) (Supplemental Figure 1). The Bacon age-depth model we present below was used to assign the zone ages in Figure 3 and Supplemental Figure 2. Pollen concentrations averaged 13,700 ± 8,800 grains/$cm^3$ from 15,700–12,900 cal yr BP, increased to 43,600 ± 12,400 grains/$cm^3$ from 12,900–12,000 cal yr BP, and then fell to an average of 28,000 ± 18,000 grains/$cm^3$ from 11,700–9,100 cal yr BP (Fig. 3). Pollen grains that were not determinable were most common from 15,600–14,300 cal yr BP with a maximum of 1.4% of the pollen sum. Variance along DCA axis 1 was 0.1821, and 0.1266 along DCA axis 2. DCA axis 1 displays a strong gradient from pollen types characteristic of juniper-sage woodlands (Cupressaceae and *Artemisia*) to pollen types associated with arid Alkali Sink steppe (e.g., Amaranthaceae and *Sarcobatus*). Arboreal pollen types associated with Sierran montane and subalpine forests (*Pinus*, *Tsuga mertensiana*, and *Abies*) plot about the origin. When plotted as a time series, DCA axis-1 scores indicate large compositional turnover in pollen taxa (ter Braak, 1985) highlighting periods of high landscape instability, while overall long-term trends show ecological gradients from woodland to steppe (Fig. 4).

Pollen Zone A (15,700 cal yr BP to 14,700 cal yr BP) was dominated by *Pinus* pollen (~40–80%), with high *Artemisia*, Cupressaceae, and *Quercus* pollen all between 10–15%. *Sequoiadendron*-type pollen and *Sporormiella* fungal spores both peaked at ~4% of the terrestrial pollen sum, the highest of the entire record from the core. Cyperaceae pollen abundance in Zone A was also the highest of the record (~5%). Alkali Sink pollen taxa (Amaranthaceae and *Sarcobatus*) were relatively high (~5%), while lowland herb pollen (Poaceae, Asteraceae, and *Ambrosia*) had a combined abundance of <4%. Microcharcoal influx was low, with values averaging 65 particles/$cm^2$/yr. DCA axis-1 scores for samples from this zone generally plot near the origin, influenced by high Cyperaceae and *Quercus*.

In Pollen Zone B (14,700 cal yr BP to 14,000 cal yr BP), *Artemisia, Salix, Ceanothus*, lowland herb pollen, and microcharcoal influxes all abruptly increased between two pollen samples 8 cm apart at ca. 14,800 cal yr BP (Fig. 4). The age-depth model indicates these two samples are 100 ± 40 yr apart. Coevally, Amaranthaceae and *Sarcobatus* pollen abundances dropped to ~3%, and *Sporormiella* abundance fell to ≤1%. *Tsuga mertensiana* pollen become consistently present at ~1% abundance. *Quercus*, *Sequoiadendron*-type, and *Abies* pollen remained relatively unchanged throughout the interval. At 14,100 cal yr BP, pollen from lowland herbs increased to 7% and *Artemisia* peaked at 37%, the highest of the core record. Cupressaceae pollen increased to 14%, and microcharcoal influx increased to 240 particles/$cm^2$/yr at the end of the zone.

https://doi.org/10.1017/qua.2022.70 Published online by Cambridge University Press

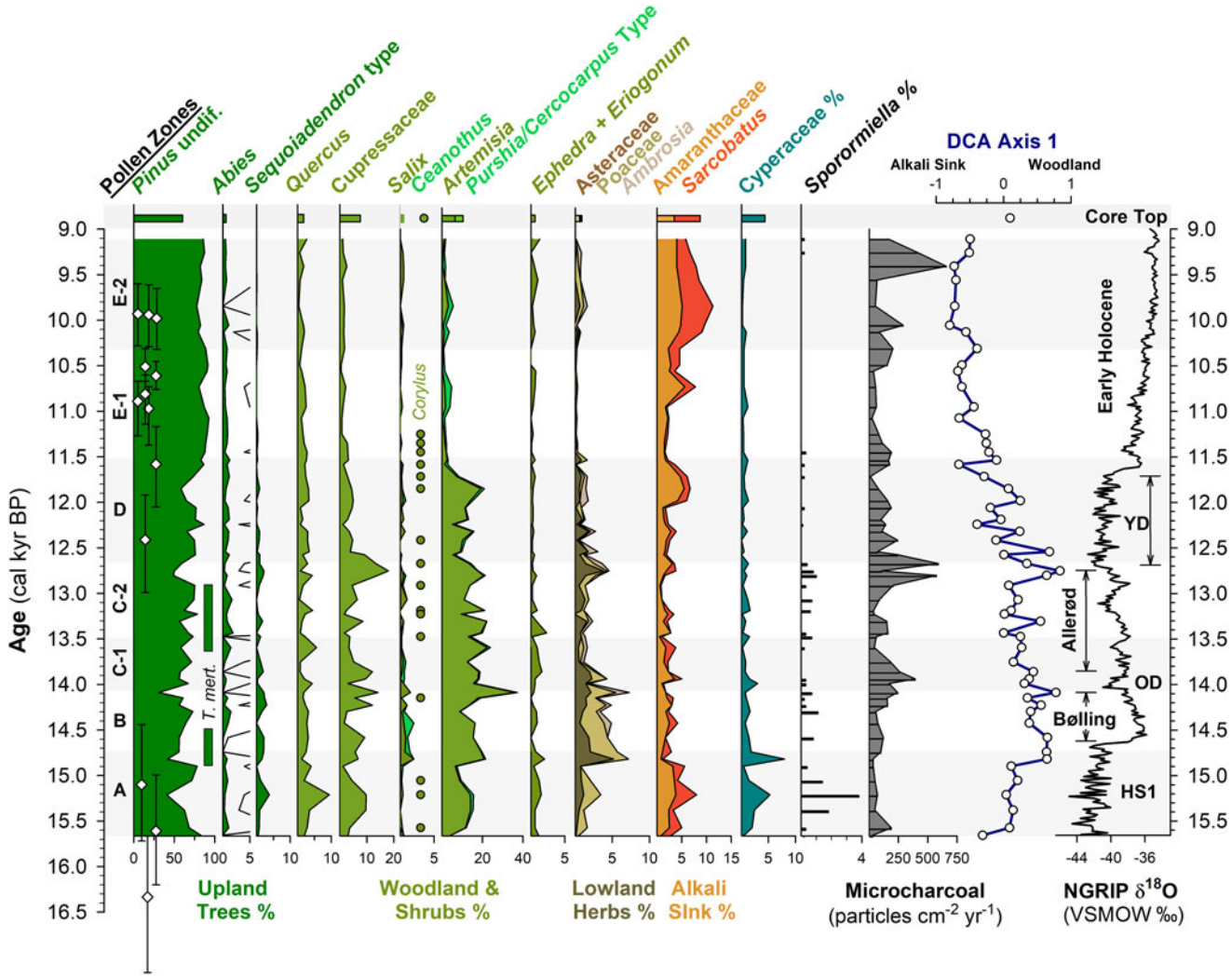


**Figure 4.** Summary MONO15 pollen diagram compared to DCA axis-1 scores (Supplemental Figure 4) and the Greenland NGRIP $\delta^{18}O$ record (Rasmussen et al., 2006). Pollen zones were denoted based on CONISS analysis (Supplemental Figure 1). Dark green bars represent the presence (~1%) of *Tsuga mertensiana* (*T. mert*) pollen and dots indicate the presence of *Corylus* pollen. White diamonds show MONO15 radiocarbon dates with 2-sigma uncertainties (updated from Hodelka et al., 2020; Fig. 3). Black-lined abundance curves are exaggerated by 10%. HS1—Heinrich Stadial 1, OD—Older Dryas, YD—Younger Dryas.

Zone C (14,000 cal yr BP to 12,700 cal yr BP) was divided into two subzones: C1 (14,000–13,400 cal yr BP) and C2 (13,400–12,700 cal yr BP). The age model had low precision in this interval because there were no age control points (Fig. 4). Early in Zone C1, microcharcoal peaked to ~390 pieces particles/cm$^2$/yr and lowland herb pollen fell to 2%. *Ceanothus* and *Salix* pollen abundance dropped to <1%. Cupressaceae pollen abundance declined from 9% to 4% at the end of Zone C1. *Sporormiella* spores were not consistently present in Zone C1 and did not exceed 0.5% of the pollen sum. In Zone C2, *Eriogonum* and *Ephedra* pollen fell to <1%. Both *Tsuga mertensiana* pollen and *Sporormiella* spores became consistently present in the record again at ≤1% abundance, and *Corylus* pollen was present. Cupressaceae pollen rose throughout Zone C2 from ~2% to 18%. Similarly, lowland herb pollen peaked to 4% at 12,750 cal yr BP. Microcharcoal influx increased to ~500 particles/cm$^2$/yr during the same interval.

Pollen Zone D (12,700 cal yr BP to 11,500 cal yr BP) was marked by a decline in Cupressaceae pollen from 18% to 5% between 12,700 cal yr BP and 12,500 cal yr BP, and declined thereafter to 3% at 11,500 cal yr BP. *Sequoiadendron*-type pollen abundances also declined throughout the zone from 1.5% at 12,500 cal yr BP to 0.5% at 11,500 cal yr BP. Similarly, lowland herb abundances fell from ~5% at 12,700 cal yr BP to <2% at 11,500 cal yr BP. *Sporormiella* occurrences fell at the boundary of Zone C2 and D at 12,650 cal yr BP, and occurrences thereafter were sporadic and only reached ~0.2% of the terrestrial pollen sum. Amaranthaceae and *Sarcobatus* pollen rose to 6% between 12,000 cal yr BP and 11,700 cal yr BP, while *Artemisia* pollen fell from 20% to ≤ 2% between 11,850 cal yr BP to 11,500 cal yr BP. Microcharcoal fell from 590 particles/cm$^2$/yr at 11,700 cal yr BP to 170 particles/cm$^2$/yr at 11,500 cal yr BP. DCA axis-1 scores were highly variable, but gradually decreased from 0.67 to -0.66 throughout the zone.

Pollen Zone E (11,500 cal yr BP to 9,100 cal yr BP) was divided into two subzones: E1 (11,500–10,300 cal yr BP) and E2 (10,300–9,100 cal yr BP). In Zone E1, *Pinus* pollen rose to 93% and remained consistently above 80% throughout Zone E1. Amaranthaceae and *Sarcobatus* pollen abundances averaged 3%, while Cupressaceae, *Artemisia*, and lowland herbs all remained

https://doi.org/10.1017/qua.2022.70 Published online by Cambridge University Press

below 2%. In Zone E1, the last appearance of *Sporormiella* occurred at 11,450 (11,900–11,050 cal yr BP) cal yr BP and did not reappear until 9,200 cal yr BP. In Zone E2, Amaranthaceae and *Sarcobatus* pollen abundance rose from 6% to 11% from 10,300 cal yr BP to 9,800 cal yr BP. Similarly, *Artemisia,* Cupressaceae, and lowland herb pollen all rose slightly to <5%. The last appearance of *Sequoiadendron*-type occurred at 9,600 (9,970–9,160 cal yr BP) cal yr BP. The average microcharcoal influx rose to 240 particles/cm$^2$/yr and peaked to 660 particles/cm$^2$/yr at 9,400 cal yr BP. *Sporormiella* was present in two samples in Zone E2. Compared to Zone E2, the MONO15 core-top pollen sample shows *Pinus*, Cupressaceae, *Artemisia*, and a DCA axis-1 score more similar to the Pleistocene, but abundances of *Abies*, *Purshia-Cercocarpus* type, and Alkali Sink pollen comparable to the Early Holocene. *Sequoiadendron*-type, *Tsuga mertensiana*, and *Sporormiella* are absent from the surface sediment sample.

## DISCUSSION

### *Chronology and lake-level influence on pollen interpretations*

Developing reliable chronologies for proxies from arid, closed-basin lakes such as Mono Lake is a challenging problem for Quaternary studies (Zimmerman et al., 2019). The carbon cycle within the lake produces significant reservoir effects (Peng and Broecker, 1980), and precludes the possibility of reliably radiocarbon dating bulk sediments (Zimmerman et al., 2019. Moreover, the MONO15 core is located ~1 km from the modern western shoreline, making terrestrial plant macrofossils rare, particularly during the late Pleistocene highstands (Hodelka et al., 2020). We have attempted to compensate for the paucity of terrestrial macrofossils by using flow cytometry to concentrate and purify pollen extracts for radiocarbon dating (Zimmerman et al., 2019; Tunno et al., 2021; Fig. 3). Moreover, lithologic changes have been carefully observed, and apparent deposition of turbidites and tephra have been incorporated into the age-depth model (Hodelka et al., 2020; Fig. 3). While the MONO15 age model returns relatively high uncertainties, the overall sedimentation rate during the deglacial period is well-constrained by three basal ages, and shows that the overall sampling interval of the pollen record is between ca. 100 to 200 years per pollen sample, which is high-resolution enough to characterize the response of rapid events during the late Pleistocene (Anderson et al., 2022).

Another challenge for interpretating fossil pollen assemblages from the large pluvial lakes of the Great Basin are the large pollen source areas, which potentially complicate ecological and climate interpretations. For example, as the lakes changed in depth and spatial extent during the last deglaciation (e.g., Ibarra et al., 2014; Rehis et al., 2014), lower elevations were alternately inundated or exposed. This could have affected pollen assemblages by changing the relative proportion of lowland to highland pollen influx to the core site. In the Mono Basin, the expansive, flat-lying lowlands rapidly became exposed as the shoreline fell from late glacial to modern levels, potentially complicating ecological interpretations (Fig. 5).

To examine the effects of lake-level dynamics on the vegetation signal, we compare our MONO15 deep-water pollen record to the littoral pollen record of Davis (1999a) and the paleoshoreline elevation through the last deglaciation (Ali, 2018). The core studied by Davis (1999a) was taken in less than 3 m water depth on the delta of Post Office Creek. Given the position of the core on a delta in front of steep drainages of the Sierran flank, we expect that the fossil pollen assemblage of that core had a smaller overall source area, biased to the hillslopes and the creek upslope of the delta. In contrast, the MONO15 core was collected from the local depositional center of Mono Lake within the western embayment, and likely integrates a greater source area from the surrounding lowlands and highlands to the north and south. Three pollen types (Cupressaceae, *Artemisia*, and Amaranthaceae) and *Sporormiella* spores from both cores and the MONO15 $\delta^{13}C_{OC}$ profile (Hodelka et al., 2020) illustrated lake-level effects on lowland vegetation (Fig. 5D).

The only substantial regression of Mono Lake indicated by both pollen records is the Early Holocene regression, when nearly 50% of the basin became subaerially exposed compared to the late Pleistocene highstand (after Ali, 2018; Fig. 5). Both pollen records show a gradual decline in Cupressaceae pollen from 13,000 cal yr BP to 11,000 cal yr BP at this transition. Given the different pollen source areas for each sediment core, the same pattern in both records likely indicates a basin-wide reduction in Cupressaceae independent of lake level. The corresponding rise in Amaranthaceae pollen in both pollen spectra records the regional expansion of Amaranthaceae and other halophyte vegetation onto newly exposed lowlands. Moreover, the $\delta^{13}C_{TOC}$ profile records an increase from −28‰ to −24‰ across the Younger Dryas–Holocene transition, also likely capturing an expansion of C4 *Atriplex* spp. (Amaranthaceae; Fig. 5).

However, the temporal pattern of *Artemisia* pollen in both cores differs substantially, implying differing source areas of *Artemisia* pollen. In the MONO15 record, there is a dramatic, ca. 300-year-long decrease (250–370 yr, 95% confidence interval) in *Artemisia* pollen to near zero percent that began at 11,850 cal yr BP. The littoral record shows no such decline. The disconnect between the two core records suggests that the decline in *Artemisia* pollen abundances in the MONO15 core was driven by the lake-level regression because it would have increased the distance between *Artemisia* steppe and the lake shore and increased the area for other lowland plant colonization (i.e., Amaranthaceae). In the littoral core, constant high *Artemisia* abundances likely resulted from continued proximity of the core site to the steep flanks of the Sierra Nevada, where *Artemisia* from higher elevations still grew despite the substantial lake regression. Therefore, the decrease in *Artemisia* in MONO15 does not indicate a major, basin-wide extirpation of *Artemisia* (Fig. 5). The rapid decline in *Artemisia* in the MONO15 pollen record following the rapid lake regression at the Younger Dryas termination indicates a shift in the pollen source area of the deep-water MONO15 core in the earliest Holocene.

However, the late Pleistocene MONO15 pollen record appears less strongly influenced by lake-level dynamics than the early Holocene. Although the overlap of the two pollen records ends early in the Younger Dryas, the deglacial-age lake was consistently higher than its Holocene average (Ali, 2018), and the morphology of the basin dictates that the changes in the proportions of low- and high-elevation shorelands were small compared to the post-Younger Dryas recession (Fig. 5). Similarly, the $\delta^{13}C_{TOC}$ and the C:N record indicate far less influence from terrestrial vegetation (Hodelka et al., 2020). Thus, it is more likely that changes in the MONO15 pollen were more strongly influenced by direct changes in climate or ecological interactions than by autogenic effects of lake-level fluctuations until the end of the Pleistocene.

https://doi.org/10.1017/qua.2022.70 Published online by Cambridge University Press

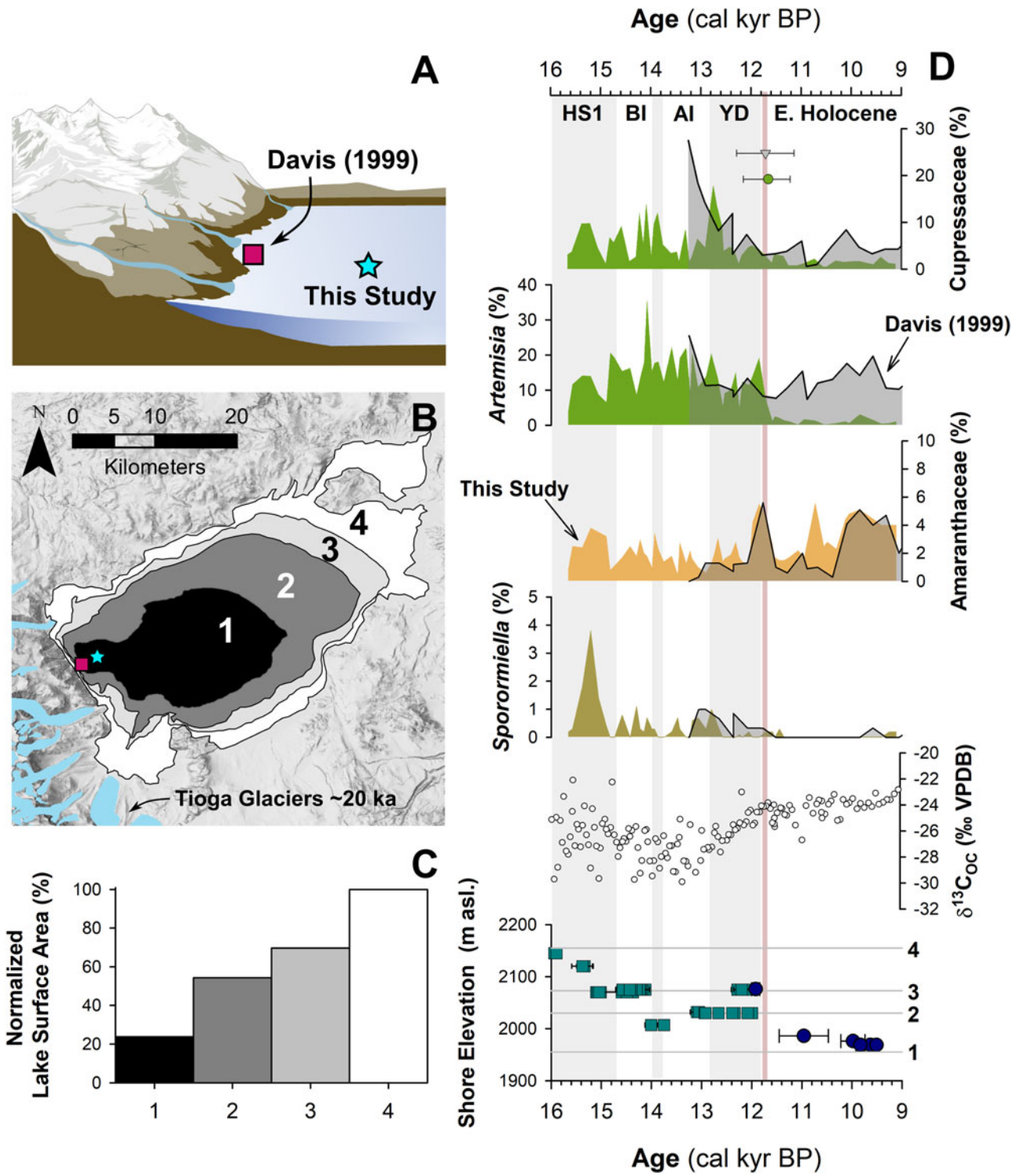


**Figure 5.** Relationship between lake level and pollen assemblages: (A) cartoon of the eastern Sierra Front and Mono Lake showing the coring locations of Davis (1999) and MONO15 (this study) during the late Pleistocene (after Hodelka et al., 2020); (B) lake-surface extent at major terraces (numbered 1–5); (C) percent changes in surface area normalized to the Pleistocene highstand at ca. 16,000 cal yr BP for each major terrace; (D) comparison of Cupressaceae, *Artemisia*, Amaranthaceae, and *Sporormiella* palynomorph abundances and temporal patterns between the MONO15 and Davis (1999; gray shading) cores compared to MONO15 $\delta^{13}C_{OC}$ (Hodelka et al., 2020), and lake level during the deglacial period (Ali, 2018). Teal squares show U-Series dates and blue circles show radiocarbon dates (Ali, 2018). The numbered elevation lines on the Mono Lake hydrograph in panel D correspond to lake extent and surface area of panels B and C, respectively. Both the littoral and offshore pollen records show good agreement in relative palynomorph abundances and temporal patterns except for *Artemisia* pollen at the onset of the Holocene at ca. 11,700 cal yr BP, which is coeval to the largest drop in lake level. Modeled age uncertainties of the Pleistocene–Holocene boundary (light pink line) are shown for both the Davis core (grey triangle) and the MONO15 core (green circle); m asl–m above sea level. HS1—Heinrich Stadial 1, BI—Bølling Interstade, AI—Allerød Interstade, YD—Younger Dryas.

https://doi.org/10.1017/qua.2022.70 Published online by Cambridge University Press

## Terrestrial ecosystem development around Mono Lake

### Community composition

The MONO15 pollen assemblage records a mixed vegetation community of Sierran (e.g., *Abies*, *Corylus*, *Tsuga mertensiana*, and *Sequoiadendron*-type), Great Basin (e.g., *Ephedra* and *Sarcobatus*), and cosmopolitan (e.g., *Artemisia*, *Ambrosia*, Poaceae) taxa around Mono Lake during the last deglaciation. The dominance of *Pinus*, *Artemisia*, and Cupressaceae pollen in the MONO15 core suggests that extensive woodlands surrounded the lake during the late Pleistocene. However, establishing the species composition of the Pleistocene woodlands around Mono Lake is difficult due to the low taxonomic resolution of both *Pinus* and Cupressaceae pollen. *Pinus* pollen identified in the MONO15 record was dominantly *P.* subg *Pinus* (diploxylon) type, suggesting the Sierran taxa *Pinus jeffreyi* and *P. contorta* var. *murrayana* (Anderson and Davis, 1988). Less common occurrences of *Pinus* subg. *strobus* (haploxylon) type could include *P. flexis*, *P. albicaulis*, or *P. monticola* (Hansen and Cushing, 1973; Anderson and Davis, 1988). Macrofossil evidence shows all of the *Pinus* species mentioned above were present in the eastern Sierra Nevada since at least the Early Holocene (Anderson, 1990a, 1996). It is unlikely *Pinus monophyla* was a source of haploxylon pollen to Mono Lake because macrofossil evidence suggests that this species was confined further south, and first appeared on Bodie Hills around the Middle Holocene (Nowak et al., 1994; Halford, 1998; Cole et al., 2013).

Cupressaceae pollen taxonomy is also difficult to infer (Bouchal and Denk, 2020) because multiple species of *Juniperus* as well as *Calocedrus decurrens* are present in the Sierra Nevada/Mono Lake region. On the Volcanic Tablelands 60 km south of Mono Lake, *Juniperus osteosperma* has been present since at least ca. 20,000 cal yr BP at 1,300 m asl (Jennings and Elliot-Fisk, 1993). Both *Juniperus osteosperma* and *J. occidentalis* macrofossils are found in late Pleistocene middens from around Winnemucca Lake (Lake Lahontan basin; Thompson et al., 1986; Nowak et al., 1994), 230 km north of Mono Lake. To our knowledge, there are no late Pleistocene macrofossil studies that have been conducted closer to Mono Lake, which makes it difficult to further clarify the origin of Cupressaceae pollen. However, both juniper species are found in Mono Basin today at different elevations along with the smaller shrub *Juniperus communis*. It is possible that both juniper trees co-occurred around Mono Lake similar to the Lahontan Basin (Thompson et al., 1986).

### The curious case of giant sequoia

The presence of *Sequoiadendron*-type pollen at Mono Lake during the late Pleistocene is an intriguing biogeographic enigma (Davis, 1999a; this study). During the Miocene to early Pliocene, *Sequoiadendron* was common throughout much of the Great Basin (Axelrod, 1986), but at present, *Sequoiadendron* is confined to only ~70 small groves in the western Sierra Nevada between 1400 m and 2200 m elevation (Hartesveldt et al., 1975). These groves are fragmented into two distinct zones. The southern zone, from 35°N to 36.5°N, contains most individuals in larger groves, while the northern zone contains just a few isolated and small groves up to 39°N (Hartesveldt et al., 1975; Fig. 1). Mono Lake sits over the Sierra Crest east of the northern *Sequoiadendron* zone and ~70 km from the nearest modern *Sequoiadendron* grove. Despite the isolated geographic distribution, Davis (1999a) surprisingly reported *Sequoiadendron*-type pollen from Mono Lake during the latest Pleistocene at values of ≤20% of the terrestrial pollen sum, similar values to those from modern groves (Anderson, 1990b). In our deep-water MONO15 record, *Sequoiadendron*-type pollen was also consistently present, but at ≤5% abundance. The consistent presence of *Sequoiadendron*-type pollen across the Sierra Crest near the very fragmented and isolated northern end of its modern range hints at major biogeographic reorganizations of this iconic species.

Here, we present and discuss two plausible hypotheses to explain the presence of *Sequoiadendron*-type pollen: (1) the pollen was locally produced within ~10s of kilometers of Mono Lake, or (2) the pollen was produced by expanded populations of *Sequoiadendron* in the western Sierra Nevada and transported 70–100s of kilometers across the Sierra Crest. Evidence in favor of a local population includes a limited number of studies that have shown *Sequoiadendron* pollen is only locally dispersed within ~1–10 km of the individual trees. Anderson (1990b) examined the modern pollen rain surrounding two *Sequoiadendron* groves, and showed limited pollen dispersal within a kilometer of the grove boundaries. More recently, a genetic study by DeSilva and Dodd (2020) has echoed the pollen rain findings of Anderson (1990b), and indicated that the genetic connectivity (i.e., pollen dispersal) between *Sequoiadendron* trees is limited to 6–11 km, depending on the size of the groves. The high abundance of *Sequoiadendron*-type pollen at Mono Lake and poor pollen dispersal of *Sequoiadendron* as shown by Anderson (1990b) led Davis (1999a) to suggest the possibility that Pleistocene refugial populations of *Sequoiadendron* existed in the eastern Sierra Nevada until the warm and drier Early Holocene. These modern analog studies, although limited, would suggest the high abundances of *Sequoiadendron*-type pollen within Mono Lake were produced by nearby *Sequoiadendron* trees.

However, other pollen records from near Mono Lake (e.g., Black Lake, Barrett Lake, Tioga Pass Pond; Fig. 1) do not record *Sequoiadendron*-type pollen during the terminal Pleistocene (Batchelder, 1970; Anderson, 1990a). The only other Pleistocene occurrence of *Sequoiadendron*-type pollen in the eastern Sierra Nevada is at Owens Lake, where Woolfenden (2003) reported sporadic *Sequoiadendron*-type pollen over the last 180,000 years, including during the last deglaciation. The sporadic occurrences in the Owens Lake record are more likely to be the result of long-distance transport because nearby middens clearly show that Great Basin-like vegetation assemblages of *Juniperus* spp. and *Pinus monophylla* dominated the valley floor (Koehler and Anderson, 1994). Yet, at the higher elevation and more-northward Mono Lake, conditions for *Sequoiadendron* may have been more tolerable. During the Pleistocene, the major limiting factor for potential *Sequoiadendron* populations at Mono Lake was likely minimum temperatures because this determines the modern upper-elevation limit of modern *Sequoiadendron* groves (Hartesvedlt et al., 1975). The modern groves have mean annual temperatures between 7–12°C, close to those of the Mono Basin at present (Fig. 2), while chironomid temperature reconstructions from Hidden Lake, 50 km north and 300 m higher than Mono Lake, show a 3°C temperature decrease during the last deglaciation (Potito et al., 2006), still potentially within the tolerance of *Sequoiadendron*. Given that the eastern Sierra Nevada has far steeper and, consequently, smaller zonal stratification along elevation than the gently sloping western Sierra, any potential *Sequoiadendron* individuals would have been confined to small refugia.

The alternative hypothesis is that *Sequoiadendron* pollen was transported at least ~100 km across the Sierra Crest during the

https://doi.org/10.1017/qua.2022.70 Published online by Cambridge University Press

late Pleistocene, facilitated by expanded populations, stronger westerly or southwesterly winds, and a more open landscape during the late Pleistocene. Pollen and macrofossil records from King's Canyon, Nicholas Meadows, and Exchequer Meadows show that *Sequoiadendron* had an expanded distribution during the late Pleistocene in the western Sierra Nevada (Cole, 1983; Davis and Moratto, 1988; Koehler and Anderson, 1994), potentially down to the Sierran foothills where pollen was transported to Tulare Lake in the San Joaquin Valley (Davis, 1999b). Furthermore, *Sequoiadendron* pollen is small (20–30 µm) and could theoretically be transported longer distances than modern observations suggest if environmental conditions were favorable. For example, if southwesterly winds were common, just to the south of Mono Lake, the San Joaquin ridge of the Sierra Crest is lower than much of the surrounding divide and could allow for long-distance transport of pollen across the glaciated Sierra Nevada.

Other pollen types, particularly bisaccate gymnosperm pollen such as that from *Pinus* and other prolific pollen producers like *Quercus,* must have been transported across the divide as well under such conditions. However, the DCA ordination shows *Pinus* and *Quercus* pollen plot opposite *Sequoiadendron* about the origin, suggesting the taxa have inversely related abundances (Supplemental Figure 4). This is reflected in the biostratigraphy because *Pinus* is less common during the Pleistocene ($\bar{x}$ = 65%) than the Holocene ($\bar{x}$ = 86%), while pollen types almost certainly reflecting local vegetation are proportionally higher during the Pleistocene (e.g., *Artemisia* and *Sarcobatus*; Figs. 4, 5). Similarly, *Quercus* has relatively constant abundances in the MONO15 core, suggesting a constant influx of long-distance-transported pollen, while *Sequoiadendron*-type pollen abundance gradually declines until extirpation from the record at ca. 9,500 cal yr BP.

Without additional evidence, particularly from plant macrofossils, we cannot draw a definitive conclusion. In either scenario, the consistent presence of *Sequoiadendron*-type pollen in the MONO15 record for over 6,000 years during deglaciation has important implications for the biogeographic history of the species because few pollen records are available from nearby disjointed, northern groves (Fig. 1). The extirpation of *Sequoiadendron*-type pollen at Tulare Lake between 10,000 and 9,000 cal yr BP (Davis, 1999b; Fig. 1A) is remarkably similar in timing to the Mono Lake records (Davis, 1999a; this study), and suggests a major contraction in the distribution of *Sequoiadendron* associated with the Holocene transition. Future work on characterizing a fundamental climate niche for *Sequoiadendron* and a better understanding of its pollen and seed dispersal could also help clarify this enigma. Given that *Sequoiadendron* grove boundaries have remained largely static or even contracted since their discovery by Euro-Americans in the 1850s (Stephenson, 1994), it may be that Late Holocene environmental conditions already exceeded *Sequoiadendron*'s preferred climate niche well before the onset of the Anthropocene warming.

### *Ecosystem development during deglaciation*

The MONO15 pollen record demonstrates distinct sensitivities of vegetation to both rapid and orbitally paced climate change (Figs. 4, 6). Prior studies have shown clear connections between hydroclimate change in the central Sierra Nevada and Pacific Ocean conditions (Benson et al., 2003; Potito et al., 2006; Street et al., 2012). However, in the central Sierra Nevada, vegetation responses to the rapid hydroclimate changes of the last deglaciation have remained unclear or muted (Mensing, 2001; MacDonald et al., 2008). At Mono Lake, DCA axis-1 scores, when plotted as a time series, capture a gradual decline of wooded lowland communities dominated by *Pinus* and Cupressaceae, and replacement by more arid Amaranthaceae- and *Sarcobatus*-dominated steppe. This pattern was likely a response to increased summer temperatures and the gradual northward migration of winter storm tracks across coastal California following the retreat of the Laurentide and Cordilleran Ice Sheets (Kirby et al., 2013; Feakins et al., 2019; Fig. 6).

The basal ca. 1,000 years of the pollen record (15,600 cal yr BP to 14,700 cal yr BP) show low pollen and microcharcoal concentrations, which suggests vegetated areas within Mono Basin were likely reduced because of recently deglaciated canyons (Rood et al., 2011) and lowlands inundated by a highstand of Mono Lake at ca. 16,000 cal yr BP (Ali, 2018). Unglaciated highlands around Mono Lake were likely dominated by alpine and subalpine communities, consistent with Great Basin plant macrofossil data showing subalpine vegetation assemblages from 1,800 m asl to 2,200 m asl. (Thompson, 1990). Elevated Amaranthaceae, *Sarcobatus*, and Cyperaceae pollen suggests a patchwork of Alkaline Sink steppe and marshes developed within the basin as the lake gradually regressed from the highstand until ca. 14,000 cal yr BP (Ali, 2018; Fig. 6). The presence of *Quercus* and *Corylus* pollen in this interval suggests nearby chaparral on dry soils. High *Sporormiella* abundances indicate relatively high megafauna activity around the lake from 15,400 cal yr BP to 15,000 cal yr BP, perhaps tracking the progressive increase in lowland vegetation.

DCA axis 1 shows major turnover of pollen taxa between two samples taken 8 cm apart at 904 cm to 896 cm composite-core depth, when pollen concentrations and microcharcoal influxes increased. The age-depth model indicates an age of 14,800 (15,400–14,200 cal yr BP) cal yr BP for these samples, although the chronological control in that interval of the core is poor. The appearance of *Tsuga mertensiana* and *Ceanothus* pollen suggests the establishment of montane forest communities within the basin (Anderson and Davis, 1988). Similarly, lowland herb and shrub pollen of plants found in woodland understories (Barbour et al., 2007), such as Poaceae, *Ambrosia*, and Asteraceae, also increased. We find no evidence of a sedimentary hiatus between the two samples, suggesting this major vegetation turnover occurred rapidly. It could potentially record a response to the onset of rapid warming and hydroclimate changes of the Bølling interstadial, the influence of which has been documented by paleoclimate records throughout the western US (e.g., Oster et al., 2009, 2015; Wagner et al., 2010; Heusser et al., 2015; Feakins et al., 2019). Paleoshoreline records show Mono Lake stabilized during much of the Bølling interval (Ali, 2018), probably because of higher influx of glacial meltwater from retreating Tioga glaciers (Schaefer et al., 2006; Rood et al., 2011) balancing the increased evaporation. As a result, riparian zones featuring *Salix* also expanded (Fig. 4). The decrease in *Sporormiella* likely reflected a reduction in the activity of megafauna around the lake. A peak in microcharcoal and a spike in *Artemisia* and Cupressaceae pollen at 14,100 (14,700–13,500 cal yr BP) cal yr BP could record a brief signal of ecosystem change in response to the short, Older Dryas stade, although it is seen in only one pollen sample (Fig. 6).

The brief rise in Cupressaceae pollen between ca. 12,800 cal yr BP to 12,500 cal yr BP may reflect an expansion of *Juniperus* woodlands near the onset of the Younger Dryas due to an

https://doi.org/10.1017/qua.2022.70 Published online by Cambridge University Press

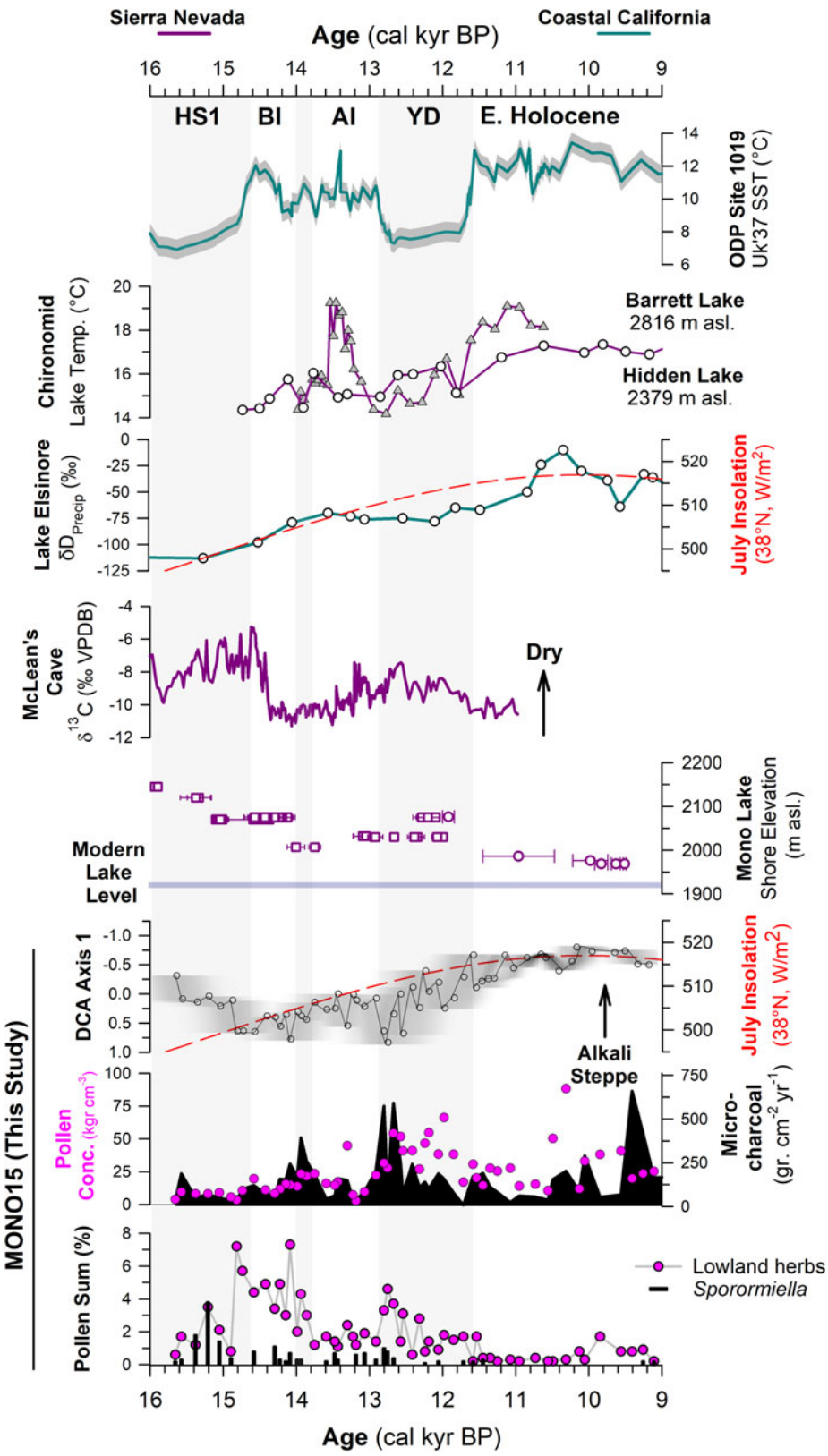


**Figure 6.** Comparison of regional hydroclimate proxies and the MONO15 record. Records from the Sierra Nevada are purple and pink, and marine and coastal records are teal. From top to bottom: sea-surface temperature (SST) record from ODP site 1019 (Barron et al., 2003; Praetorius et al., 2020); chironomid temperature records from Barrett Lake, California (MacDonald et al., 2008) and Hidden Lake, California (Potito et al., 2006); leaf-wax δD record from Lake Elsinore, California, indicating gradual northward migration of winter storms (Kirby et al., 2013; Feakins et al., 2019); speleothem $\delta^{13}C$ record of moisture from McLean's Cave, California (Oster et al., 2015); Mono Lake hydrograph during deglaciation (Ali, 2018) with squares (U-series) and circles (radiocarbon). Results from the MONO15 core, DCA axis-1 time series with the age-model uncertainty of the core superimposed (grey shading); microcharcoal influx (black shading) and pollen concentrations (pink dots); lowland herb pollen (Asteraceae, Poaceae, and *Ambrosia* pollen) and *Sporormiella* abundance. Gray bars indicate cold periods from the NGRIP $\delta^{18}O$ record (Rasmussen et al., 2006). HS1—Heinrich stadial 1, BI—Bølling interstadial, AI—Allerød interstadial, YD—Younger Dryas stade.

increase in precipitation and decrease in temperatures, which is shown by hydroclimate proxies nearby at Barrett Lake and Starkweather Pond (MacDonald et al., 2008). A peak in microcharcoal is also observed near the onset of the Younger Dryas, similar to other records in the western US (Marlon et al., 2009). However, the overall trend in pollen turnover, reflected by DCA axis 1, shows the Younger Dryas to be a transitional period consisting of two distinct phases. DCA axis-1 scores show high

https://doi.org/10.1017/qua.2022.70 Published online by Cambridge University Press

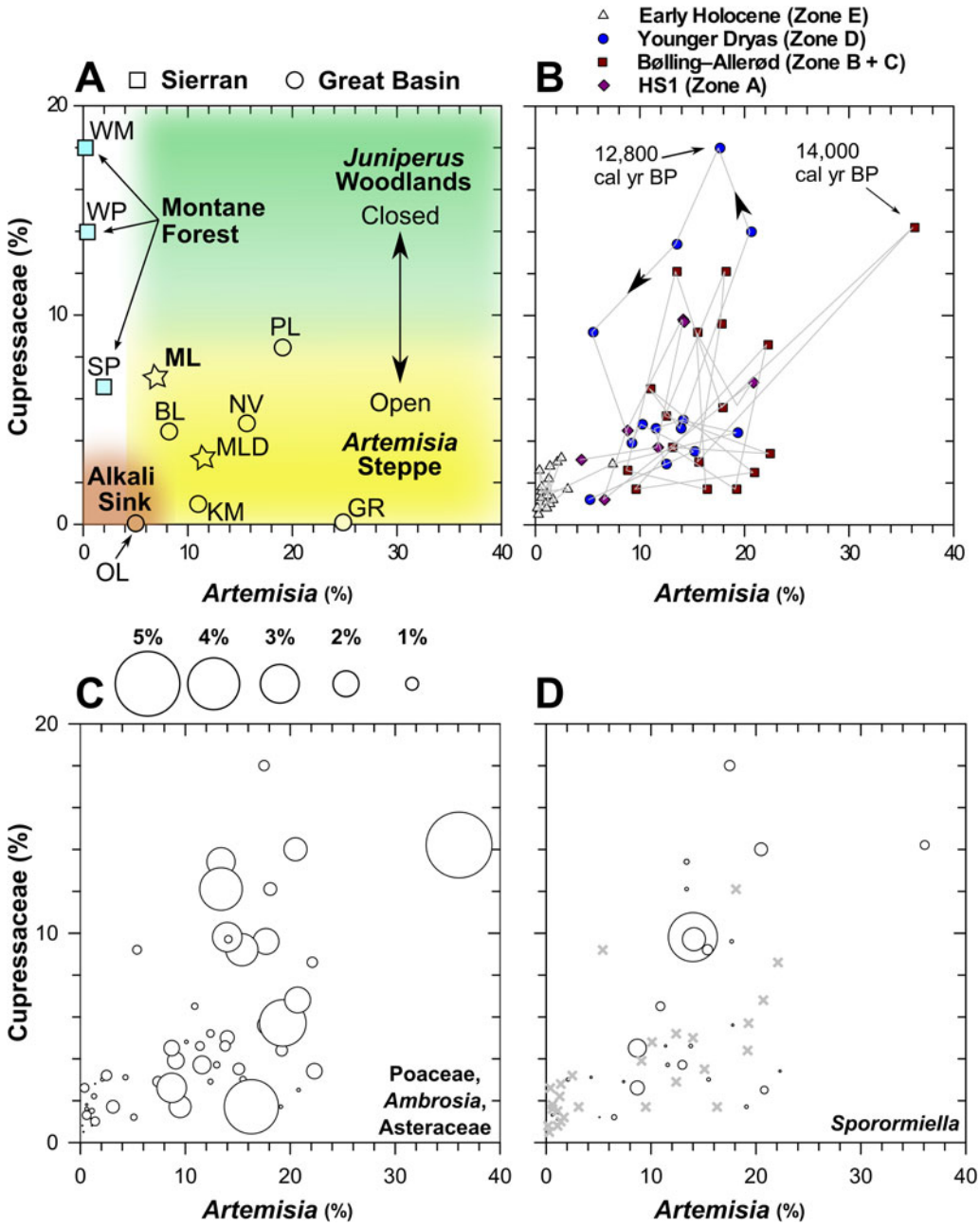


**Figure 7.** The relationship between *Artemisia* and Cupressaceae pollen at Mono Lake and regional sites in the Great Basin and Sierra Nevada. (A) Conceptual diagram for interpretating the relative dominance and canopy dynamics of *Juniperus* woodlands and *Artemisia* Steppe defined by regional lake and wetland core-top pollen abundances. Stars indicate the modern pollen spectrum at Mono Lake (ML, this study; MLD, Davis, 1999a). (B) MONO15 pollen data showing inferred *Juniperus* and *Artemisia* canopy dynamics through the last deglaciation, HS1—Heinrich stadial 1. (C) MONO15 herbaceous pollen taxa (Poaceae, *Ambrosia*, and Asteraceae) of each sample plotted as bubble sizes, reflecting understory plants. (D) MONO15 *Sporormiella* abundances plotted as bubble size; x symbols show pollen samples with no *Sporormiella*. At Mono Lake, Cupressaceae pollen increased after major increases in microcharcoal during the onset of stadial events such as the Younger Dryas (ca. 12,800 cal yr BP) and Older Dryas (ca. 14,000 cal yr BP). BL—Black Lake, GR—Gund Ranch, KM—Kingston Meadow, NV—Newark Valley Pond, OL—Owens Lake, PL—Pyramid Lake, SP—Starkweather Pond, WM—Wawona Meadow, WP— Woski Pond.

pollen turnover from 12,800 cal yr BP to 12,000 cal yr BP. A second possible phase occurred from ca. 12,500 cal yr BP to 11,500 cal yr BP, when Amaranthaceae and *Sarcobatus* pollen increased. *Sporormiella* abundance also declines at the onset of the Younger Dryas, indicating an extirpation of many megafauna herbivores, and is consistent with the last appearance datum of many megafauna species throughout the western US (Grayson, 2016).

From 11,500–10,300 cal yr BP (Zone E2), the MONO15 pollen record was probably autogenically influenced by the lake regression (Ali, 2018). However, the extirpation of *Sequoiadendron*-type and *Corylus* pollen shown in both the MONO15 and Davis (1999a) cores probably reflects the end of chaparral and Sierran montane vegetation communities near Mono Basin. Cupressaceae pollen abundance fell below modern levels (Fig. 4), indicating a decline in *Pinus-Juniperus* woodlands within the basin, perhaps resembling

https://doi.org/10.1017/qua.2022.70 Published online by Cambridge University Press

the very heterogenous distribution found in the Late Holocene (Constantine, 1993). From 10,300 cal yr BP to the end of the pollen record at 9,100 cal yr BP, several pollen types increase slightly, including Amaranthaceae, *Sarcobatus*, *Artemisia*, and *Purshia-Cercocarpus* type, all suggesting the dominance of semiarid vegetation like that found today (Fig. 4). Prior studies at high-elevation lakes in the eastern Sierra Nevada show that Early Holocene vegetation communities were open, wooded environments dominated by *Pinus*, *Quercus*, and shrubs, also suggesting dispersal upslope and stratification of vegetation previously found in Mono Basin (Anderson, 1990a; Davis, 1999a; MacDonald et al., 2008). Early Holocene dryness has been observed throughout the Sierra Nevada and Great Basin (Davis and Moratto, 1988; Anderson and Smith, 1994; Mensing, 2001; Brugger and Rhode, 2020), based on the decline in mesophilic arboreal taxa at lower elevations and the establishment of the semiarid vegetation assemblages seen today. Similarly, the complete absence of *Sporormiella* from 11,500–9,200 cal yr BP captures the final extirpation of Pleistocene megafauna in the basin, also consistent with the last appearance dates of megafauna fossils found in the Great Basin (Grayson, 2006).

### *Climate change effects on canopy dynamics and megafauna*

Around Mono Lake, the response of the terrestrial ecosystem to climate transitions was characterized by rapid changes in the relative abundances of *Pinus*, Cupressaceae, *Artemisia*, and herbaceous pollen (Poaceae, Asteraceae, and *Ambrosia*). These pollen types represent the major constituents of lowland, wooded ecosystems, and their variability likely captures reorganization of the canopy structure in response to hydroclimate changes. In particular, the increase in Cupressaceae and herbaceous pollen produce similar patterns to climate transitions documented in isotope records in California at McLean's Cave (Oster et al., 2015), Barrett Lake (MacDonald et al., 2008), and Lake Elsinore (Heusser et al., 2015). Large peaks in microcharcoal at ca. 14,000 cal yr BP and ca. 12,900 cal yr BP suggest that these vegetation changes were associated with more wildfires around Mono Lake.

A proposed scheme for understanding the dynamics of Pleistocene *Juniperus* woodlands around Mono Lake and their decline into the early Holocene is shown in Figure 7. Modern pollen assemblages from core-top samples from throughout the western Great Basin and Sierra Nevada (Table 1) show low Cupressaceae pollen abundances (<5%), reflecting the sparse patchwork of modern juniper-pinyon woodlands interspersed within *Artemisia* steppe on Great Basin landscapes today (Fig. 7A). The abundance of *Artemisia* pollen reflects the presence of *Artemisia* plants within the sagebrush steppe. *Artemisia* pollen abundances are near zero in the drier, lower elevation Alkali Sink steppe, and increase to nearly 20% in sagebrush-dominated environments.

In stark contrast, late Pleistocene MONO15 samples show Cupressaceae pollen abundances of 20%, particularly during the early phase of the Younger Dryas and Bølling-Allerød interstadial (Fig. 7B). During these periods, Cupressaceae abundances fluctuated while *Artemisia* pollen abundances remained relatively constant. This suggests that *Juniperus* woodlands expanded and contracted within an otherwise sagebrush-dominated landscape, resulting in alternately more open- or closed-canopy structure around Mono Lake. During events such as the early Younger Dryas, an increase in charcoal is followed by an increase in Cupressaceae pollen (Fig. 7B). More frequent burning of sagebrush steppe likely resulted in increased abundances of herbaceous types like Poaceae, Asteraceae, and *Ambrosia* (Fig. 7C). This suggests that greater effective moisture provided more fuel to enhance fire activity, followed by a rapid expansion of juniper at the expense of sagebrush, a process that is ongoing in the modern Great Basin (Romme et al., 2009).

Major vegetation and climate change during the last deglaciation has also been invoked to explain the decline and extinction of Pleistocene megafauna in North America (Gill et al., 2009; Faith, 2011; Meltzer, 2015). The early Holocene contraction of *Juniperus* woodlands would have put pressure on megafauna populations as food resources found in the woodland ecosystem declined. Lowland herb and shrub pollen abundances during periods of high *Artemisia* and Cupressaceae pollen imply that most of the pollen was produced by understory plants growing within the juniper-sage communities (Fig. 7C). *Sporormiella* decreased in two steps at 14,800 (15,400–14,200 cal yr BP) cal yr BP and 12,800 (13,200–12,100 cal yr BP) cal yr BP before its last appearance at 11,500 (11,900–11,050 cal yr BP) cal yr BP. The timing suggests a connection with vegetation and wildfire changes observed in the pollen record, implying climate and vegetation change may have been the major drivers of the megafauna decline near the onset of the Bølling interstade and Younger Dryas. For example, after the *Sporormiella* decline, lowland herb (*Artemisia*, Asteraceae, and Poaceae) and shrub (*Artemisia* and *Ceanothus*) pollen rapidly increased in abundance. This pollen abundance increase could indicate a release from intensive herbivory (e.g., Gill et al., 2009; Fig. 6). Prior work from the Great Basin has suggested that megafauna populations were low in comparison to the Mojave Desert to the south (Grayson, 2016). This appears to be reflected in limited *Sporormiella* presence in pollen studies from Great Basin wetlands (e.g., Gund Ranch; Brugger and Rhode, 2020). Yet, the high and relatively consistent presence of *Sporormiella* in Mono Lake sediments indicates higher megafauna activity, and implies that the rim of the Great Basin and Sierra Nevada may have provided more suitable habitats for megafauna than the central Great Basin.

## CONCLUSIONS

The MONO15 core pollen record documents both multimillennial and centennial responses of vegetation, fire, and megafauna activity to major environmental changes around Mono Lake from 15,600–9,100 cal yr BP. The pollen record documents the presence of a mixed assemblage of Sierran and Great Basin plants around Mono Lake during the late Pleistocene, likely supporting substantial populations of mammalian megafauna. Comparison to a littoral record by Davis (1999a) suggests minimal influence of lake level on the pollen record until the Early Holocene. Moreover, both pollen records feature the consistent presence of *Sequoiadendron*-type pollen, hinting at an expanded Pleistocene *Sequoiadendron* population. *Pinus*- and Cupressaceae-dominated woodlands and *Artemisia* steppe surrounding Mono Lake gradually declined and retreated to higher elevations as temperatures increased and available moisture decreased into the Early Holocene, tracking higher summer insolation. However, this gradual transition was punctuated by periods of rapid structural changes in *Pinus-Juniperus-Artemisia* communities as wildfire activity and hydroclimate rapidly changed landscape openness. These vegetation and wildfire changes appear to have had major effects on megafauna activity surrounding Mono Lake. *Sporormiella* declined in a stepwise fashion at 14,800 (15,400–14,200 cal yr BP) cal yr BP and 12,800

https://doi.org/10.1017/qua.2022.70 Published online by Cambridge University Press

(13,200–12,100 cal yr BP) cal yr BP before its disappearance at 11,500 (11,900–11,050 cal yr BP) cal yr BP, all associated with episodes of major vegetation and wildfire changes. Although the age-depth model has relatively high uncertainties during the late Pleistocene, the succession of vegetation communities and turnover mirrors that of the onset of the Bølling-Allerød interstadial, Younger Dryas, and the Early Holocene recognized from regional speleothems and other geochemical records. Overall, the late Pleistocene *Pinus-Juniperus-Artemisia* communities around Mono Lake proved resistant to rapid climate change and increased wildfire while Pleistocene conditions of high available moisture remained. However, the onset of sustained dryness and higher summer temperatures during the Early Holocene produced major biogeographic changes, replacing the mixed wooded Sierran and Great Basin vegetation with the more zonal modern communities of sagebrush and Alkaline Sink steppe.

**Acknowledgments.** We thank the LacCore Facility for core curation and processing guidance. We are grateful to R.S. Anderson and the members of the Penn State Paleobiology Seminar for discussion, and G.H. Ali for providing lake-level data and constructive comments on early drafts of the manuscript. We thank two anonymous reviewers and Wyatt Oswald and Nicholas Lancaster for their feedback, and our friend O.K. Davis for inspiration.

**Financial Support.** This work was supported by funding from The Pennsylvania State University, the University of Kentucky, and NSF award 1829093. Radiocarbon dating was conducted at Lawrence Livermore National Laboratory under grant 17-ERD-052 to S.R.H. Zimmerman; this is LLNL-JRNL-820887.

**Data Availability Statement.** All palynological and geochronology data from the MONO15 core will be submitted to the Neotoma Paleoecological Database for public access.

**Supplementary Material.** The Supplementary Material for this article can be found at https://doi.org/10.1017/qua.2022.70

## REFERENCES

**Ali, G.**, 2018. *Late Glacial and Deglacial Fluctuations of Mono Lake, California*. PhD dissertation, Columbia University, New York, USA.

**Ali, G.A.H., Lin, K., Hemming, S.R., Cox, S.E., Ruprecht, P., Zimmerman, S.R.H., Stine, S., Wang, X.**, 2022. Emergence of wet conditions in the Mono Basin of the Western USA coincident with inception of the Last Glaciation. *Geological Society of America Bulletin* **134**, 2267–2279.

**Anderson, L., Wahl, D.B., Bhattacharya, T.**, 2022. Understanding rates of change: a case study using fossil pollen records from California to assess the potential for and challenges to a regional data synthesis. *Quaternary International* **621**, 26–36.

**Anderson, R.S.**, 1990a. Holocene forest development and paleoclimates within the central Sierra Nevada, California. *Journal of Ecology* **78**, 470–489.

**Anderson, R.S.**, 1990b. Modern pollen rain within and adjacent to two giant sequoia (*Sequoiadendron giganteum*) groves, Yosemite and Sequoia national parks, California. *Canadian Journal of Forest Research* **20**, 1289–1305.

**Anderson, R.S.**, 1996. Postglacial biogeography of Sierra lodgepole pine (*Pinus contorta* var. *murrayana*) in California. *Écoscience* **3**, 343–351.

**Anderson, R.S., Carpenter, S.L.**, 1991. Vegetation change in Yosemite Valley, Yosemite National Park, California, during the protohistoric period. *Madroño* **38**, 1–13.

**Anderson, R.S., Davis, O.K.**, 1988. Contemporary pollen rain across the central Sierra Nevada, California, USA: relationship to modern vegetation types. *Arctic and Alpine Research* **20**, 448–460.

**Anderson, R.S., Smith, S.J.**, 1994. Paleoclimatic interpretations of meadow sediment and pollen stratigraphies from California. *Geology* **22**, 723–726.

**Anderson, R.S., Stillick, R.D., Jr.**, 2013. 800 years of vegetation change, fire and human settlement in the Sierra Nevada of California, USA. *The Holocene* **23**, 823–832.

**Axelrod, D.I.**, 1986. The Sierra redwood (*Sequoiadendron*) forest: end of a dynasty. *Geophytology* **16**, 25–36.

**Bailey, R.A.**, 2004. Eruptive history and chemical evolution of the precaldera and postcaldera basaltic-dacite sequences, Long Valley, California: implications for magma sources, current magmatic unrest, and future volcanism. *United States Geological Survey Professional Paper* **1692**, 76 p.

**Barbour, M., Keeler-Wolf, T., Schoenherr, A.A.**, 2007. *Terrestrial Vegetation of California, 3rd Edition*. University of California Press, Berkeley.

**Barron, J.A., Heusser, L., Herbert, T., Lyle, M.**, 2003. High-resolution climatic evolution of coastal northern California during the past 16,000 years: *Paleoceanography* **18**, 1020. https://doi.org/10.1029/2002PA000768.

**Batchelder, G.L.**, 1970. *Postglacial Ecology at Black Lake, Mono County, California*. PhD dissertation, Arizona State University, Tempe, USA.

**Benson, L., Linsley, B., Smoot, J., Mensing, S., Lund, S., Stine, S., Sarna-Wojcicki, A.**, 2003. Influence of the Pacific Decadal Oscillation on the climate of the Sierra Nevada, California and Nevada. *Quaternary Research* **59**, 151–159.

**Benson, L.V., Lund, S.P., Burdett, J.W., Kashgarian, M., Rose, T.P., Smoot, J.P., Schwartz, M.**, 1998. Correlation of Late-Pleistocene lake-level oscillations in Mono Lake, California, with North Atlantic Climate Events. *Quaternary Research* **49**, 1–10.

**Blaauw, M., Christen, J.A.**, 2011. Flexible paleoclimate age-depth models using an autoregressive gamma process. *Bayesian Analysis* **6**, 457–474.

**Bouchal, J.M., Denk, T.**, 2020. Low taxonomic resolution of papillate Cupressaceae pollen (former Taxodiaceae) impairs their applicability for palaeo-habitat reconstruction. *Grana* **59**, 71–93.

**Brady, R.T.**, 2011. Obsidian source distribution and prehistoric settlement patterns at Mono Lake, Eastern California. *Journal of California and Great Basin Anthropology* **31**, 3–24.

**Brugger, S.O., Rhode, D.**, 2020. Impact of Pleistocene–Holocene climate shifts on vegetation and fire dynamics and its implications for Prearchaic humans in the central Great Basin, USA. *Journal of Quaternary Science* **35**, 987–993.

**Clark, P.U., Shakun, J.D., Baker, P.A., Bartlein, P.J., Brewer, S., Brook, E., Carlson, A.E., *et al.***, 2012. Global climate evolution during the last deglaciation. *Proceedings of the National Academy of Sciences* **109**, E1134–E1142. https://doi.org/10.1073/pnas.1116619109.

**Cole, K.**, 1983. Late Pleistocene vegetation of Kings Canyon, Sierra Nevada, California. *Quaternary Research* **19**, 117–129.

**Cole, K.L., Fisher, J.F., Ironside, K., Mead, J.I., Koehler, P.**, 2013. The biogeographic histories of *Pinus edulis* and *Pinus monophylla* over the last 50,000 years. *Quaternary International* **310**, 96–110.

**Constantine, H.**, 1993. *Plant Communities of the Mono Basin*. The Mono Lake Committee Natural History Field Guide Series, Kutzavi Press, Lee Vining, California.

**Davis, O.K.** 1999a. Pollen analysis of a Late-Glacial and Holocene sediment core from Mono Lake, Mono County, California. *Quaternary Research* **52**, 243–249.

**Davis, O.K.** 1999b. Pollen analysis of Tulare Lake, California: Great Basin-like vegetation in central California during the full-glacial and early Holocene. *Review of Palaeobotany and Palynology* **107**, 249–257.

**Davis, O.K., Anderson, R.S., Fall, P.L., O'Rourke, M.K., Thompson, R.S.**, 1985. Palynological evidence for Early Holocene aridity in the southern Sierra Nevada, California. *Quaternary Research* **24**, 322–332.

**Davis, O.K., Moratto, M.J.** 1988. Evidence for a warm dry early Holocene in the western Sierra Nevada of California: pollen and plant macrofossil analysis of Dinkey and Exchequer meadows. *Madroño*, 132–149.

**Davis, O.K., Shafer, D.S.**, 2006. *Sporormiella* fungal spores, a palynological means of detecting herbivore density. *Palaeogeography, Palaeoclimatology, Palaeoecology* **237**, 40–50.

**Denton, G.H., Anderson, R.F., Toggweiler, J.R., Edwards, R.L., Schaefer, J.M., Putnam, A.E.**, 2010. The last glacial termination. *Science* **328**, 1652–1656.

**DeSilva, R., Dodd, R.S.**, 2020. Fragmented and isolated: Limited gene flow coupled with weak isolation by environment in the paleoendemic giant sequoia (*Sequoiadendron giganteum*). *American Journal of Botany* **107**, 45–55.

**Faegri, K., Kaland, P.E., Krzywinski, K.**, 1989. *Textbook of Pollen Analysis, 4th Edition*. John Wiley & Sons Ltd., Chichester.

**Faith, J.T.**, 2011. Late Pleistocene climate change, nutrient cycling, and the megafaunal extinctions in North America. *Quaternary Science Reviews* **30**, 1675–1680.

**Feakins, S.J., Wu, M.S., Ponton, C., Tierney, J.E.**, 2019. Biomarkers reveal abrupt switches in hydroclimate during the last glacial in southern California. *Earth and Planetary Science Letters* **515**, 164–172.

**Gillespie, A.R., Clark, D.H.**, 2011. Chapter 34—Glaciations of the Sierra Nevada, California, USA. In: Ehlers, J., Gibbard, P.L., Hughes, P.D., Eds., *Quaternary Glaciations - Extent and Chronology: A Closer Look. Developments in Quaternary Sciences Vol. 15*, Elsevier, Amsterdam, pp. 447–462.

**Gill, J.L., Williams, J.W., Jackson, S.T., Donnelly, J.P., Schellinger, G.C.**, 2012. Climatic and megaherbivory controls on late-glacial vegetation dynamics: a new, high-resolution, multi-proxy record from Silver Lake, Ohio. *Quaternary Science Reviews* **34**, 66–80.

**Gill, J.L., Williams, J.W., Jackson, S.T., Lininger, K.B., Robinson, G.S.**, 2009. Pleistocene megafaunal collapse, novel plant communities, and enhanced fire regimes in North America. *Science* **326**, 1100–1103.

**Glover, K.C., Chaney, A., Kirby, M.E., Patterson, W.P., MacDonald, G.M.**, 2020. Southern California vegetation, wildfire, and erosion had nonlinear responses to climatic forcing during Marine Isotope Stages 5–2 (120–15 ka). *Paleoceanography and Paleoclimatology* **35**, e2019PA003628. https://doi.org/10.1029/2019PA003628.

**Glover, K.C., George, J., Heusser, L., MacDonald, G.M.**, 2021. West Coast vegetation shifts as a response to climate change over the past 130,000 years: geographic patterns and process from pollen data. *Physical Geography* **42**, 542–560.

**Grayson, D.**, 2011. *The Great Basin: A Natural Prehistory, Revised and Expanded Edition*. University of California Press, Berkeley.

**Grayson, D.**, 2016. *Giant Sloths and Sabertooth Cats: Extinct Mammals and the Archaeology of the Ice Age Great Basin*. University of Utah Press, Salt Lake City.

**Grayson, D.K.**, 2006. The Late Quaternary biogeographic histories of some Great Basin mammals (western USA). *Quaternary Science Reviews* **25**, 2964–2991.

**Grimm, E.C.**, 1987. CONISS: A FORTRAN 77 program for stratigraphically constrained cluster analysis by the method of incremental sum of squares. *Computers & Geosciences*, **13**, 13–35.

**Halford, F.K.**, 1998 *Archaeology and Environment on the Dry Lakes Plateau, Bodie Hills, California: Hunter-Gatherer Coping Strategies for Holocene Environmental Variability*. Master's thesis, University of Nevada, Reno, USA.

**Hansen, B.S., Cushing, E.J.**, 1973. Identification of pine pollen of Late Quaternary Age from the Chuska Mountains, New Mexico. *Geological Society of America Bulletin* **84**, 1181–1200.

**Hartesveldt, R.J., Harvey, H.T., Shellhammer, H.S., Stecker, R.E.**, 1975. *The Giant Sequoia of the Sierra Nevada*. U.S. Department of the Interior, National Park Service, Washington, D.C.

**Heusser, L.E., Kirby, M.E., Nichols, J.E.**, 2015. Pollen-based evidence of extreme drought during the last Glacial (32.6–9.0 ka) in coastal southern California. *Quaternary Science Reviews* **126**, 242–253.

**Hodelka, B.N., McGlue, M.M., Zimmerman, S., Ali, G., Tunno, I.**, 2020. Paleoproduction and environmental change at Mono Lake (eastern Sierra Nevada) during the Pleistocene-Holocene transition. *Palaeogeography, Palaeoclimatology, Palaeoecology* **543**, 109565. https://doi.org/10.1016/j.palaeo.2019.109565.

**Hudson, A.M., Hatchett, B.J., Quade, J., Boyle, D.P., Bassett, S.D., Ali, G., De los Santos, M.G.**, 2019. North-south dipole in winter hydroclimate in the western United States during the last deglaciation. *Scientific Reports* **9**, 4826. https://doi.org/10.1038/s41598-019-41197-y

**Ibarra, D.E., Egger, A.E., Weaver, K.L., Harris, C.R., Maher, K.**, 2014. Rise and fall of late Pleistocene pluvial lakes in response to reduced evaporation and precipitation: evidence from Lake Surprise, California. *Geological Society of America Bulletin* **126**, 1387–1415.

**Jellison, R., Melack, J.M.**, 1993. Algal photosynthetic activity and its response to meromixis in hypersaline Mono Lake, California. *Limnology and Oceanography* **38**, 818–837.

**Jennings, S.A., Elliott-Fisk, D.L.**, 1993. Packrat midden evidence of Late Quaternary vegetation change in the White Mountains, California-Nevada. *Quaternary Research* **39**, 214–221.

**Kapp, R.O., Davis, O.K., King, J.E.**, 2000. *Ronald O. Kapp's Pollen and Spores, Second Edition*. American Association of Stratigraphic Palynologists Foundation, College Station, Texas.

**Kirby, M.E., Feakins, S.J., Bonuso, N., Fantozzi, J.M., Hiner, C.A.**, 2013. Latest Pleistocene to Holocene hydroclimates from Lake Elsinore, California. *Quaternary Science Reviews* **76**, 1–15.

**Koehler, P.A., Anderson, S.R.**, 1994. The paleoecology and stratigraphy of Nichols Meadow, Sierra National Forest, California, USA. *Palaeogeography, Palaeoclimatology, Palaeoecology* **112**, 1–17. https://doi.org/10.1016/0031-0182(94)90132-5

**Lachniet, M.S., Denniston, R.F., Asmerom, Y., Polyak, V.J.**, 2014. Orbital control of western North America atmospheric circulation and climate over two glacial cycles. *Nature Communications* **5**, 3805. https://doi.org/10.1038/ncomms4805.

**Lajoie, K.**, 1968. *Quaternary Stratigraphy and Geologic History of Mono Basin*. PhD thesis, University of California, Berkeley.

**Lyle, M., Heusser, L., Ravelo, C., Andreasen, D., Olivarez Lyle, A., Diffenbaugh, N.**, 2010. Pleistocene water cycle and eastern boundary current processes along the California continental margin. *Paleoceanography* **25**, PA4211. https://doi.org/10.1029/2009PA001836

**MacDonald, G.M., Moser, K.A., Bloom, A.M., Porinchu, D.F., Potito, A.P., Wolfe, B.B., Edwards, T.W.D., Petel, A., Orme, A.R., Orme, A.J.**, 2008. Evidence of temperature depression and hydrological variations in the eastern Sierra Nevada during the Younger Dryas Stade. *Quaternary Research* **70**, 131–140.

**Mack, R.N., Thompson, J.N.**, 1982. Evolution in steppe with few large, hooved mammals. *The American Naturalist* **119**, 757–773.

**Marlon, J.R., Bartlein, P.J., Walsh, M.K., Harrison, S.P., Brown, K.J., Edwards, M.E., Higuera, P.E., *et al.***, 2009. Wildfire responses to abrupt climate change in North America. *Proceedings of the National Academy of Sciences* **106**, 2519–2524. https://doi.org/10.1073/pnas.0808212106.

**McAndrews, J.H., Berti, A.A., Norris, G.**, 1973. *Key to the Quaternary Pollen and Spores of the Great Lakes Region*. Royal Ontario Museum Life Sciences Miscellaneous Publications, Ottowa.

**Meltzer, D.J.**, 2015. Pleistocene overkill and North American mammalian extinctions. *Annual Review of Anthropology* **44**, 33–53.

**Mensing, S.A.**, 2001. Late-Glacial and Early Holocene vegetation and climate change near Owens Lake, eastern California. *Quaternary Research* **55**, 57–65.

**Mensing, S., Smith, J., Burkle Norman, K., Allan, M.**, 2008. Extended drought in the Great Basin of western North America in the last two millennia reconstructed from pollen records. *Quaternary International* **188**, 79–89.

**Millar, C.I., King, J.C., Westfall, R.D., Alden, H.A., Delany, D.L.**, 2006. Late Holocene forest dynamics, volcanism, and climate change at Whitewing Mountain and San Joaquin Ridge, Mono County, Sierra Nevada, CA, USA. *Quaternary Research* **66**, 273–287.

**Minckley, T.A., Bartlein, P.J., Whitlock, C., Shuman, B.N., Williams, J.W., Davis, O.K.**, 2008. Associations among modern pollen, vegetation, and climate in western North America. *Quaternary Science Reviews* **27**, 1962–1991.

**Nowak, C.L., Nowak, R.S., Tausch, R.J., Wigand, P.E.**, 1994. Tree and shrub dynamics in northwestern Great Basin woodland and shrub steppe during the Late-Pleistocene and Holocene. *American Journal of Botany* **81**, 265–277.

**O'Keefe, J.M.K., Wymer, C.L.**, 2017. An alternative to acetolysis: Application of an enzyme-based method for the palynological preparation of fresh pollen, honey samples and bee capsules. *Palynology* **41**, 117–120.

**Oksanen, F., Blanchet, G., Friendly, M., Kindt, R., Legendre, P., McGlinn, D., Minchin, P.R., *et al.***, 2019. *vegan: Community Ecology Package*. R package version **2**.5-7. https://CRAN.R-project.org/package=vegan

**Oster, J.L., Montañez, I.P., Santare, L.R., Sharp, W.D., Wong, C., Cooper, K.M.** 2015. Stalagmite records of hydroclimate in central California during termination 1. *Quaternary Science Reviews* **127**, 199–214.

**Oster, J.L., Montañez, I.P., Sharp, W.D., Cooper, K.M.**, 2009. Late Pleistocene California droughts during deglaciation and Arctic warming. *Earth and Planetary Science Letters* **288**, 434–443.

**Oswald, W.W., Foster, D.R., Shuman, B.N., Doughty, E.D., Faison, E.K., Hall, B.R., Hansen, B.C.S., Lindbladh, M., Marroquin, A., Truebe, S.A.**, 2018. Subregional variability in the response of New England vegetation to postglacial climate change. *Journal of Biogeography* **45**, 2375–2388.

https://doi.org/10.1017/qua.2022.70 Published online by Cambridge University Press

**Peng, T.-H., Broecker, W.**, 1980. Gas exchange rates for three closed-basin lakes. *Limnology and Oceanography* **25**, 789–796.

**Potito, A.P., Porinchu, D.F., MacDonald, G.M., Moser, K.A.**, 2006. A late Quaternary chironomid-inferred temperature record from the Sierra Nevada, California, with connections to northeast Pacific sea surface temperatures. *Quaternary Research* **66**, 356–363.

**Praetorius, S.K., Condron, A., Mix, A.C., Walczak, M.H., McKay, J.L., Du, J.**, 2020. The role of Northeast Pacific meltwater events in deglacial climate change. *Science Advances* **6**, eaay2915. https://doi.org/10.1126/sciadv.aay2915.

**PRISM Climate Group**, 2014. Oregon State University, https://prism.oregonstate.edu. Data created February 4, 2014; accessed December 16, 2020.

**Putnam, W.C.**, 1950. Moraine and shoreline relationships at Mono Lake, California. *Geological Society of America Bulletin* **61**, 115–122.

**Rasmussen, S.O., Andersen, K.K., Svensson, A.M., Steffensen, J.P., Vinther, B.M., Clausen, H.B., Siggaard-Andersen, M.-L., *et al.***, 2006. A new Greenland ice core chronology for the last glacial termination. *Journal of Geophysical Research: Atmospheres* **111**, D06102. https://doi.org/10.1029/2005JD006079.

**Reheis, M.C., Adams, K.D., Oviatt, C.G., Bacon, S.N.**, 2014. Pluvial lakes in the Great Basin of the western United States—a view from the outcrop. *Quaternary Science Reviews* **97**, 33–57.

**Romme, W.H., Allen, C.D., Bailey, J.D., Baker, W.L., Bestelmeyer, B.T., Brown, P.M., Eisenhart, K.S., *et al.***, 2009. Historical and modern disturbance regimes, stand structures, and landscape dynamics in piñon–juniper vegetation of the western United States. *Rangeland Ecology & Management* **62**, 203–222.

**Rood, D.H., Burbank, D.W., Finkel, R.C.**, 2011. Chronology of glaciations in the Sierra Nevada, California, from $^{10}$Be surface exposure dating. *Quaternary Science Reviews* **30**, 646–661.

**Russell, I.C.**, 1889. Quaternary history of Mono Valley, California. In: *Eighth Annual Report of the United States Geological Survey 1886–1887, Part 1*. Government Printing Office, Washington, D.C. pp. 261–394.

**Schaefer, J.M., Denton, G.H., Barrell, D.J.A., Ivy-Ochs, S., Kubik, P.W., Andersen, B.G., Phillips, F.M., Lowell, T.V., Schlüchter, C.**, 2006. Near-synchronous interhemispheric termination of the Last Glacial Maximum in mid-latitudes. *Science* **312**, 1510–1513.

**Schols, P., Es, K., D'Hondt, C., Merckx, V., Smets, E., Huysmans, S.**, 2004. A new enzyme-based method for the treatment of fragile pollen grains collected from herbarium material. *TAXON* **53**, 777–782.

**Shuman, B.N., Newby, P., Donnelly, J.P.**, 2009. Abrupt climate change as an important agent of ecological change in the Northeast U.S. throughout the past 15,000 years. *Quaternary Science Reviews* **28**, 1693–1709.

**Smith, S.J., Anderson, R.S.**, 1992. Late Wisconsin paleoecologic record from Swamp Lake, Yosemite National Park, California. *Quaternary Research* **38**, 91–102.

**Solomon, A.M., Silkworth, A.B.**, 1986. Spatial patterns of atmospheric pollen transport in a montane region. *Quaternary Research* **25**, 150–162.

**Stephenson, N.L.**, 1994. Long-term dynamics of giant sequoia populations: implications for managing a pioneer species. In: Aune, P.S. (technical coordinator), *Proceedings of the Symposium on Giant Sequoias: Their Place in the Ecosystem and Society, 23–25 June 1992, Visalia, California, USA*. U.S. Forest Service General Technical Report PSW-GTR-151, pp. 56–63.

**Stine, S.**, 1990. Late Holocene fluctuations of Mono Lake, eastern California. *Palaeogeography, Palaeoclimatology, Palaeoecology* **78**, 333–381.

**Street, J.H., Anderson, R.S., Paytan, A.**, 2012. An organic geochemical record of Sierra Nevada climate since the LGM from Swamp Lake, Yosemite. *Quaternary Science Reviews* **40**, 89–106.

**ter Braak, C.J.**, 1985. Correspondence analysis of incidence and abundance data: properties in terms of a unimodal response model. *Biometrics* **41**, 859–873.

**Thompson, R.S.**, 1990. Late Quaternary vegetation and climate in the Great Basin. In: Betancourt, J.L., Van Devender, T.R., Martin, P.S. (Eds.), *Packrat Middens, The Last 40,000 Years of Biotic Change*. University of Arizona Press, Tucson, pp. 200–239.

**Thompson, R.S., Benson, L., Hattori, E.M.**, 1986. A revised chronology for the last Pleistocene lake cycle in the central Lahontan Basin. *Quaternary Research* **25**, 1–9.

**Tunno, I., Zimmerman, S.H., Brown, T.A., Hassel, C.A.**, 2021. An improved method for extracting, sorting and AMS dating of pollen concentrates from lake sediment. *Frontiers in Ecology and Evolution* **9**, 668676. https://doi.org/10.3389/fevo.2021.668676.

**Wagner, J.D.M., Cole, J.E., Beck, J.W., Patchett, P.J., Henderson, G.M., Barnett, H.R.**, 2010. Moisture variability in the southwestern United States linked to abrupt glacial climate change. *Nature Geoscience* **3**, 110–113.

**Wahrhaftig, C., Stock, G.M., McCracken, R.G., Sasnett, P., Cyr, A.J.**, 2019, *Extent of the Last Glacial Maximum (Tioga) glaciation in Yosemite National Park and vicinity, California. Scale 1:100,000*. U.S. Geological Survey Scientific Investigations Map 3414.

**Wendt, J.A.F., McWethy, D B., Widga, C., Shuman, B.N.**, 2022. Large-scale climatic drivers of bison distribution and abundance in North America since the Last Glacial Maximum. *Quaternary Science Reviews* **284**, 107472. https://doi.org/10.1016/j.quascirev.2022.107472.

**Whitmore, J., Gajewski, K., Sawada, M., Williams, J.W., Shuman, B., Bartlein, P.J., Minckley, T., *et al.***, 2005. Modern pollen data from North America and Greenland for multi-scale paleoenvironmental applications. *Quaternary Science Reviews* **24**, 1828–1848.

**Williams, J.W., Grimm, E.C., Blois, J.L., Charles, D.F., Davis, E.B., Goring, S.J., Graham, R.W., *et al.***, 2018. The Neotoma Paleoecology Database, a multiproxy, international, community-curated data resource. *Quaternary Research* **89**, 156–177.

**Winkler, D.W.**, Ed., 1977. *An Ecological Study of Mono Lake, California*. Institute of Ecology Publication 12, University of California, Davis.

**Woolfenden, W.B.**, 2003. A 180,000-year pollen record from Owens Lake, CA: terrestrial vegetation change on orbital scales. *Quaternary Research* **59**, 430–444.

**Zimmerman, S.R.H., Brown, T.A., Hassel, C., Heck, J.**, 2019. Testing pollen sorted by flow cytometry as the basis for high-resolution lacustrine chronologies. *Radiocarbon* **61**, 359–374.

**Zimmerman, S.R.H., Hemming, S.R., Hemming, N.G., Tomascak, P.B., Pearl, C.**, 2011a. High-resolution chemostratigraphic record of late Pleistocene lake-level variability, Mono Lake, California. *Geological Society of America Bulletin* **123**, 2320–2334.

**Zimmerman, S.R.H., Hemming, S.R., Starratt, S.W.** 2021. Holocene sedimentary architecture and paleoclimate variability at Mono Lake, California. In: Starratt, S.W, Rosen, M.R. (Eds.), *From Saline to Freshwater: The Diversity of Western Lakes in Space and Time*. Geological Society of America Special Papers 536, Geological Society of America, Boulder, Colorado.

**Zimmerman, S.R.H., Pearl, C., Hemming, S.R., Tamulonis, K., Hemming, N.G., Searle, S.Y.**, 2011b. Freshwater control of ice-rafted debris in the last glacial period at Mono Lake, California, USA. *Quaternary Research* **76**, 264–271.

**Zimmerman, S.R.H., Wahl, D.B.**, 2020. Holocene paleoclimate change in the western US: the importance of chronology in discerning patterns and drivers. *Quaternary Science Reviews* **246**, 106487. https://doi.org/10.1016/j.quascirev.2020.106487.

https://doi.org/10.1017/qua.2022.70 Published online by Cambridge University Press